

# Ion chemistry and N-containing molecules in Titan's upper atmosphere

V. Vuitton<sup>a,\*</sup>, R.V. Yelle<sup>a</sup>, M.J. McEwan<sup>b</sup>

<sup>a</sup> Lunar and Planetary Laboratory, Kuiper Space Sciences Bldg, University of Arizona, 1629 E. University Blvd., Tucson, AZ 85721-0092, USA

<sup>b</sup> Department of Chemistry, University of Canterbury, Christchurch, New Zealand

Received 14 February 2007; revised 30 May 2007

Available online 15 August 2007

## Abstract

High-energy photons, electrons, and ions initiate ion–neutral chemistry in Titan's upper atmosphere by ionizing the major neutral species (nitrogen and methane). The Ion and Neutral Mass Spectrometer (INMS) onboard the Cassini spacecraft performed the first composition measurements of Titan's ionosphere. INMS revealed that Titan has the most compositionally complex ionosphere in the Solar System, with roughly 50 ions at or above the detection threshold. Modeling of the ionospheric composition constrains the density of minor neutral constituents, most of which cannot be measured with any other technique. The species identified with this approach include the most complex molecules identified so far on Titan. This confirms the long-thought idea that a very rich chemistry is actually taking place in this atmosphere. However, it appears that much of the interesting chemistry occurs in the upper atmosphere rather than at lower altitudes. The species observed by INMS are probably the first intermediates in the formation of even larger molecules. As a consequence, they affect the composition of the bulk atmosphere, the composition and optical properties of the aerosols and the flux of condensable material to the surface. In this paper, we discuss the production and loss reactions for the ions and how this affects the neutral densities. We compare our results to neutral densities measured in the stratosphere by other instruments, to production yields obtained in laboratory experiments simulating Titan's chemistry and to predictions of photochemical models. We suggest neutral formation mechanisms and highlight needs for new experimental and theoretical data.

© 2007 Elsevier Inc. All rights reserved.

**Keywords:** Atmospheres, composition; Ionospheres; Organic chemistry; Titan

## 1. Introduction

Titan is the only satellite in the Solar System with a substantial atmosphere. The pressure ranges from 1.5 bar at the surface to  $10^{-12}$  bar at 1400 km and the temperature from 70 K at the tropopause to 200 K at the stratopause (Vinatier et al., 2007). Its principal constituents are  $N_2$ , a few percent of  $CH_4$  and few tenths of a percent of  $H_2$ . Minor constituents include hydrocarbons and nitriles created by photochemistry from  $N_2$  and  $CH_4$ . The most abundant,  $C_2H_4$ ,  $C_2H_2$ , HCN and  $C_2H_6$ , have a mole fraction of a few  $10^{-6}$  in the stratosphere (Vinatier et al., 2007). They result from the action on  $N_2$  and  $CH_4$  of high-energy electrons from Saturn's magnetosphere and UV photons from solar radiation.  $CH_4$  is dissociated throughout the atmosphere, directly at higher altitudes and indirectly in the

stratosphere by photocatalytic processes. However, dissociation of  $N_2$  requires energetic electrons or photons that are deposited predominantly above  $\sim 1000$  km. It follows that formation of nitrogen-bearing molecules predominantly occurs in the upper atmosphere (Lara et al., 1996; Toubanc et al., 1995; Wilson and Atreya, 2004; Yung et al., 1984). Performing an inventory of the simpler molecules in their production region is crucial since they quickly react as they diffuse down to lower altitudes. Nitrogen can be linked to carbon at various degrees of saturation (nitriles, imines, amines) and this determines its availability for incorporation into more complex molecules. Complex N-bearing species are precursors for the creation of haze particles and can condense in the lower stratosphere (Lebonnois et al., 2002; Wilson and Atreya, 2003). Aerosols will ultimately accumulate on the surface, modifying its appearance and composition. Determination of the upper atmosphere composition is then necessary for an understanding of nitrogen chemistry at all levels of the atmosphere.

\* Corresponding author. Fax: +1 (520) 621 4933.  
E-mail address: [vvuitton@lpl.arizona.edu](mailto:vvuitton@lpl.arizona.edu) (V. Vuitton).

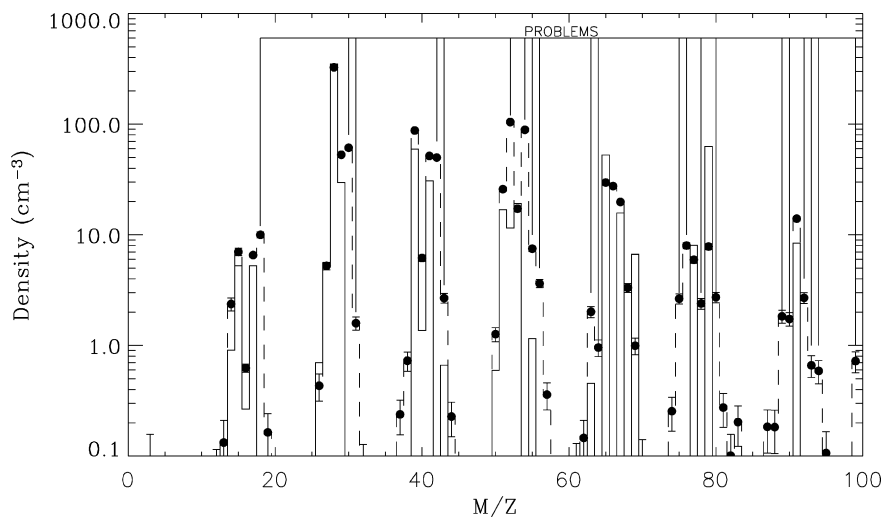


Fig. 1. INMS measurements and the Keller et al. (1998) model. The black dots show the INMS mass spectrum measured on April 16, 2005 (T5 flyby), averaged between the altitudes of 1027 and 1200 km, and the dashed line connects the points. Error bars are included with the points but are smaller than the symbol size for larger densities. They represent the uncertainty due to counting statistics and a systematic error of  $\sim 20\%$  due to calibration uncertainties. The plain line shows the model of Keller et al. (1998) scaled to match the data at  $m/z = 28$ . The mass spectrum was computed for an altitude of 1055 km using the Yung (1987) atmospheric model.

Keller et al. (1992, 1998) developed a comprehensive one-dimensional photochemical model to study both the composition and density structure of Titan's ionosphere. Their background neutral atmosphere is taken from the models developed by Toublanc et al. (1995), Yung et al. (1984) and Yung (1987). Photoionization by solar EUV and electron impact ionization by photoelectrons and saturnian magnetospheric electrons are both included. The major neutral species (nitrogen and methane) are ionized to produce  $N_2^+$ ,  $N^+$ ,  $CH_4^+$ ,  $CH_3^+$ ,  $CH_2^+$ , and  $CH^+$  ions. Ion-neutral chemistry converts these ions to higher mass products. The major species at the ionospheric peak (at an altitude of 1050 km) are found to be mostly hydrocarbon ions, such as  $C_2H_5^+$ ,  $c-C_3H_3^+$ ,  $C_3H_5^+$ , and  $C_5H_5^+$ . The only N-containing species are  $HCNH^+$  the most abundant ion,  $HC_3NH^+$  and  $C_4H_5NH^+$ . Water ion species do not reach a significant amount. Other models (Banaszekiewicz et al., 2000; Fox and Yelle, 1997; Ip, 1990; Wilson and Atreya, 2004), despite all differences in chemical networks and energy deposition processes, obtain mostly similar results.

The Ion Neutral Mass Spectrometer (INMS) onboard the Cassini spacecraft obtained measurements of Titan's ionospheric composition during the egress of the T5 encounter on 16 April, 2005. At closest approach the spacecraft was at an altitude of 1027 km, a latitude of  $74^\circ$  N, and a local time of 23:15. The solar zenith angle at this location is  $127^\circ$  and the encounter occurred in darkness. Fig. 1 shows the average ion spectrum in the 1027–1200 km region measured by INMS. The mass spectrum of Titan's ionosphere is quite complex. There are 45 peaks between  $m/z = 1$  and 99, with a mass periodicity of 12 amu. The detection threshold is roughly  $0.3 \text{ cm}^{-3}$ . A computed spectrum of Titan's ionosphere at an altitude of 1055 km based on the Keller et al. (1998) model is compared to the INMS data in Fig. 1. Although for many mass-to-charge ratios ( $m/z$ ) the ion densities are reproduced remarkably well, the measurements

show a richer composition than predicted by the model. Most of the even masses are missing.

Titan's ionospheric chemistry is simple in principle. As in any reducing environment, ionization flows from species whose parent neutrals have smaller proton affinities (PA) to species whose parent neutrals have larger PA (Fox and Yelle, 1997). It follows that the ionospheric composition is a function of the neutral composition weighted by the PA of these neutrals. Because proton exchange reactions drive the chemistry, the most abundant ions are essentially protonated neutrals (closed-shell ions). Radical cations ( $C_2H_4^+$ ,  $C_3H_4^+$ ,  $NH_3^+$ ,  $HCN^+$ ) have a low abundance because they are difficult to produce and are lost quickly through reactions with the main neutral species.

Because the atomic mass of a carbon atom is 12 amu and it has 4 valence electrons, closed-shell hydrocarbons always have an even mass. Because the atomic mass of a nitrogen atom is 14 amu and it has 5 valence electrons, closed-shell molecules containing carbon, hydrogen and a single nitrogen atom always have an odd mass. It follows that protonated closed-shell hydrocarbon ions have odd masses ( $C_xH_y + H^+$ , where  $y$  is an even integer), while ions containing a single N atom have even masses ( $C_xH_yN + H^+$ , where  $y$  is an odd integer). Thus, identifying the ions in the INMS spectra is straightforward: ions at odd values of  $m/z$  are likely protonated hydrocarbon molecules, ions at even values of  $m/z$  are likely protonated nitriles.

With this approach, Vuitton et al. (2006a) identified the previously non-attributed ions at  $m/z = 18, 30, 42, 54,$  and  $56$  as  $NH_4^+$ ,  $CH_2NH_2^+$ ,  $CH_3CNH^+$ ,  $C_2H_3CNH^+$ , and  $C_2H_5CNH^+$ , respectively. Moreover, by coupling a simple chemical model with the measured densities of ions ( $m/z < 60$ ), they determined the abundance of nine neutral species, four of them not having previously been observed on Titan.

In the following, we extend the study by Vuitton et al. (2006a) to the heavier mass end of the INMS spectrum ( $m/z > 60$ ). We use the same model as Vuitton et al. (2006a),

but extend the chemical reactions list to estimate neutral mole fractions at 1100 km for 9 new species. We discuss in more detail the production and loss reactions for the ions and how this affects the neutral densities. We compare our results to neutral densities measured in the stratosphere by other instruments, to production yields obtained in laboratory experiments simulating Titan's chemistry and to predictions of photochemical models. We suggest neutral formation mechanisms and highlight needs for new experimental or theoretical data.

In Section 2 we describe the photochemical model in detail. Section 3 focuses on ion production and loss mechanisms and neutral mole fractions. Section 4 presents and discusses comparisons with other observational, experimental and theoretical datasets. Conclusions are given in Section 5.

## 2. Theoretical model

### 2.1. Model description

The model adopts atmospheric conditions appropriate for the 1100 km level and assumes local chemical equilibrium. At this altitude, reaction rates are rapid and diffusion is unimportant by comparison. The chemical lifetime is given by  $(kN_n)^{-1}$ , where  $k$  is the ion–molecule reaction rate constant and  $N_n$  the density of reactive neutrals. A typical value for  $k$  is  $10^{-9} \text{ cm}^3 \text{ s}^{-1}$  and at 1100 km, the density of reactive neutrals is roughly  $5 \times 10^5 \text{ cm}^{-3}$ , leading to a chemical time constant of  $2 \times 10^3 \text{ s}$ . The diffusion time constant is given by  $H^2/D$ , where  $H$  is the atmospheric scale height and  $D$  the diffusion coefficient. Adopting  $H = 75 \text{ km}$  and  $D = 10^9 \text{ cm}^2 \text{ s}^{-1}$  implies a diffusion time constant of  $5 \times 10^4 \text{ s}$ , significantly longer than the chemical time constant.

The model solves the continuity equation for the  $i$ th ion species as

$$\frac{dN_i}{dt} = P_i - L_i N_i, \quad (1)$$

where  $N_i$  is the density of ion species  $i$  ( $\text{cm}^{-3}$ ), and  $P_i$  and  $L_i$  ( $\text{cm}^{-3} \text{ s}^{-1}$ ) the chemical production and loss rate, respectively.

The production rate  $P_i$  is defined as

$$P_i = \sum_n \sigma_n N_n + \sum_{i'n} \Phi_{i'n} k_{i'n} N_{i'} N_n, \quad (2)$$

where  $N_{i'}$  and  $N_n$  are the densities of other ion species  $i'$  and neutral species  $n$  ( $\text{cm}^{-3}$ ),  $\sigma_n$  is the ionization rate of neutral species  $n$  ( $\text{s}^{-1}$ ),  $\Phi_{i'n}$  is the branching ratio of the channel leading to species  $i$  and  $k_{i'n}$  is the ion–molecule rate constant ( $\text{cm}^3 \text{ s}^{-1}$ ) for the reaction between species  $i'$  and  $n$ .

The loss rate  $L_i$  is defined as

$$L_i = \alpha_i N_e N_i + \sum_n k_{in} N_i N_n, \quad (3)$$

where  $N_e$  is the electron density,  $\alpha_i$  is the electron recombination coefficient for species  $i$  ( $\text{cm}^3 \text{ s}^{-1}$ ), and  $k_{in}$  the ion–molecule rate constant ( $\text{cm}^3 \text{ s}^{-1}$ ) for the reaction between species  $i$  and  $n$ . We solve Eq. (1) by integrating to a steady state ( $dN_i/dt = 0$ ). Neutral densities  $N_n$  are held fixed with

time. We advance from one time step to the next by solving the equation with a fully implicit Newton–Raphson technique. Calculations are run until production and loss terms are balanced to better than 1 part per million.

The INMS spectra show clear signs of isotopic signatures at high  $m/z$  where the abundance of isotopic molecules is enhanced by the large number of atoms. Isotopes vary little in mass from the most abundant species. The difference in rate coefficient is usually within the experimental error. This is not true however, with isomeric species, which can have very different rate coefficients and products: e.g.,  $\text{C}_3\text{H}_3^+$ . Unfortunately, reaction rate data on most isotopic molecules is lacking. Therefore, to include the effect of isotopes we assume that the reaction rates for isotopic molecules are the same as for the main isotope. We adopt values of  $H/D = 4350$ ,  $^{12}\text{C}/^{13}\text{C} = 82.3$ , and  $^{14}\text{N}/^{15}\text{N} = 183$  based on INMS and GC–MS measurements of isotope ratios in the neutral gas (Niemann et al., 2005; Waite et al., 2005).

### 2.2. Atmospheric background

As indicated by Eqs. (2) and (3), ion densities depend closely upon the composition of the neutral atmosphere. During T5, INMS ion measurements were interspersed with neutral measurements, so the main atmospheric constituents,  $\text{N}_2$ ,  $\text{CH}_4$  and  $\text{H}_2$ , are well characterized. Their mole fraction at 1100 km are  $9.7 \times 10^{-1}$ ,  $2.7 \times 10^{-2}$  and  $4.0 \times 10^{-3}$ , respectively. Other neutral species measured by INMS include  $\text{C}_2\text{H}_2$ ,  $\text{C}_2\text{H}_6$ ,  $\text{C}_3\text{H}_4$  and  $\text{C}_3\text{H}_8$  (Waite et al., 2005). Their mole fractions for T5 appear to be similar to TA (Cui et al., in preparation). The mole fractions of these neutrals are held fixed in the model and are listed in Table 1. Other minor species have not yet been accurately constrained by INMS neutral measurements, either because their signature is masked by more abundant constituents ( $\text{C}_2\text{H}_4$ ), because of possible adsorption on the walls of the instrument (radicals,  $\text{C}_4\text{H}_2$ ,  $\text{HCN}$ , etc.), or because their density is below the detection limit. H, N and NH are fixed at values calculated in the Wilson and Atreya (2004) photochemical model. Most heavy hydrocarbons and N-containing species are best constrained by measurement of the protonated species and their densities are tuned to produce the observed ion densities. The ambient electron temperature was taken as 718 K, consistent with the value measured by the Cassini Radio Plasma Wave Spectrometer (RPWS) during the T5 encounter (Wahlund, personal communication).

### 2.3. Ionization mechanisms

Electron impact ionization of minor neutrals is slow in comparison with ion–molecule reaction rates and ionization of species other than  $\text{N}_2$  and  $\text{CH}_4$  is neglected. Adopting a photoionization cross-section of  $5 \times 10^{-16} \text{ cm}^2$  implies a photoionization time constant of  $2 \times 10^9 \text{ s}$ , much longer than the chemical time constant of  $2 \times 10^3 \text{ s}$ . For  $\text{N}_2$  and  $\text{CH}_4$  we use the electron impact ionization cross sections of Orient and Srivastava (1987) and Rapp and Englander-Golden (1965), a mean suprathermal electron energy of 100 eV (Szegő et al., 2005),

Table 1

Neutral mole fractions in Titan's atmosphere at 1100 and 300 km. The mole fractions of the species in *italic* are determined in this work from INMS neutral measurements obtained on the Cassini T5 flyby at 74° N and 1100 km. Proton affinity (Hunter and Lias, 1998) and detection in the interstellar and circumstellar medium ([http://www.astrochymist.org/astrochymist\\_ism.html](http://www.astrochymist.org/astrochymist_ism.html)) are listed as well. When a species has different isomers, the PA is that of the most stable isomer

Species	Mole fraction on Titan		Proton affinity (kJ/mol)	ISM
	1100 km	300 km		
H	$1.0 \times 10^{-3a}$	–	–	–
H <sub>2</sub>	$4.0 \times 10^{-3b}$	–	422.3	+
CH <sub>4</sub>	$2.7 \times 10^{-2b}$	$1.6 \times 10^{-2c}$	543.5	+
C <sub>2</sub> H <sub>2</sub>	$2.8 \times 10^{-4b}$	$5.0 \times 10^{-6c}$	641.4	+
<i>C<sub>2</sub>H<sub>4</sub></i>	$1.0 \times 10^{-3}$	$3.0 \times 10^{-7c}$	680.5	+
<i>C<sub>2</sub>H<sub>6</sub></i>	$1.2 \times 10^{-4b}$	$2.0 \times 10^{-5c}$	596.3	–
C <sub>3</sub> H <sub>4</sub>	$4.0 \times 10^{-6b}$	$3.0 \times 10^{-8c}$	748.0	+
C <sub>3</sub> H <sub>8</sub>	$2.3 \times 10^{-6b}$	$1.0 \times 10^{-6c}$	625.7	–
<i>C<sub>4</sub>H<sub>2</sub></i>	$1.0 \times 10^{-5}$	$1.0 \times 10^{-8c}$	737.2	+
<i>C<sub>5</sub>H<sub>4</sub></i>	$<1.0 \times 10^{-6}$	–	–	+
<i>C<sub>6</sub>H<sub>2</sub></i>	$8.0 \times 10^{-7}$	–	–	+
<i>C<sub>6</sub>H<sub>6</sub></i>	$3.0 \times 10^{-6}$	$5.0 \times 10^{-9c}$	750.4	+ <sup>d</sup>
<i>C<sub>7</sub>H<sub>4</sub></i>	$3.0 \times 10^{-7}$	–	–	+
<i>C<sub>7</sub>H<sub>8</sub></i>	$2.0 \times 10^{-7}$	–	784.0	–
<i>C<sub>8</sub>H<sub>2</sub></i>	$2.0 \times 10^{-7}$	–	–	–
N	$6.7 \times 10^{-5a}$	–	342.2	–
N <sub>2</sub>	$9.7 \times 10^{-1b}$	$9.8 \times 10^{-1c}$	493.8	+
C <sub>2</sub> N <sub>2</sub>	–	$9.0 \times 10^{-10e}$	674.7	–
<i>HCN</i>	$2.0 \times 10^{-4}$	$1.0 \times 10^{-6c}$	712.9	+
<i>CH<sub>3</sub>CN</i>	$3.0 \times 10^{-6}$	$4.0 \times 10^{-8f}$	779.2	+
<i>HC<sub>3</sub>N</i>	$4.0 \times 10^{-5}$	$4.0 \times 10^{-8e}$	751.2	+
<i>C<sub>2</sub>H<sub>3</sub>CN</i>	$1.0 \times 10^{-5}$	$<2.0 \times 10^{-9f}$	784.7	+
<i>C<sub>2</sub>H<sub>5</sub>CN</i>	$5.0 \times 10^{-7}$	$<2.0 \times 10^{-9f}$	794.1	+
<i>C<sub>4</sub>H<sub>3</sub>N</i>	$4.0 \times 10^{-6}$	–	–	+
<i>C<sub>4</sub>H<sub>5</sub>N</i>	$<3.0 \times 10^{-7}$	–	875.4	–
<i>HC<sub>5</sub>N</i>	$1.0 \times 10^{-6}$	$<4.0 \times 10^{-10f}$	–	+
<i>C<sub>5</sub>H<sub>5</sub>N</i>	$4.0 \times 10^{-7}$	–	930.0	–
<i>C<sub>6</sub>H<sub>3</sub>N</i>	$3.0 \times 10^{-7}$	–	–	+
<i>C<sub>6</sub>H<sub>7</sub>N</i>	$1.0 \times 10^{-7}$	–	949.1	–
<i>NH<sub>3</sub></i>	$6.7 \times 10^{-6}$	$<6.3 \times 10^{-9g}$	852.9	+
<i>N<sub>2</sub>H<sub>4</sub></i>	$<1.0 \times 10^{-8}$	–	853.2	–
<i>CH<sub>2</sub>NH</i>	$1.0 \times 10^{-5}$	–	853.6	+
<i>CH<sub>3</sub>NH<sub>2</sub></i>	$<1.0 \times 10^{-8}$	–	899.0	+
<i>H<sub>2</sub>O</i>	$<3.0 \times 10^{-7}$	$8.0 \times 10^{-9h}$	691.0	+
<i>H<sub>2</sub>CO</i>	–	–	712.9	+
<i>CH<sub>3</sub>OH</i>	$<3.0 \times 10^{-8}$	–	754.3	+
<i>CH<sub>3</sub>CHO</i>	$<1.0 \times 10^{-8}$	–	768.5	+
<i>CH<sub>2</sub>CO</i>	–	–	825.3	+

<sup>a</sup> Disk average predictions for solar minimum from the Wilson and Atreya (2004) photochemical model.

<sup>b</sup> INMS neutral measurements at 74° N obtained on the Cassini T5 flyby (Waite et al., 2005).

<sup>c</sup> CIRS measurements at 80° N obtained on the Cassini T3 flyby (Vinatier et al., 2007).

<sup>d</sup> Circumstellar medium only.

<sup>e</sup> CIRS measurements at 60° N obtained on the Cassini Tb flyby (Teanby et al., 2006).

<sup>f</sup> Disk average measurements obtained with the IRAM 30-m telescope (Spain) between April 1996 and December 1999 (Marten et al., 2002).

<sup>g</sup> IRIS measurements at latitudes higher than 50° N obtained during the Voyager 1 encounter in November 1980 (Bernard et al., 2003).

<sup>h</sup> Disk average measurements obtained with ISO in December 1997 (Coustenis et al., 1998).

and a CH<sub>4</sub> mole fraction of 3% (Yelle et al., 2006) to calculate the relative production rates of N<sub>2</sub><sup>+</sup>, N<sup>+</sup>, CH<sub>4</sub><sup>+</sup>, CH<sub>3</sub><sup>+</sup>, CH<sub>2</sub><sup>+</sup>, CH<sup>+</sup> and C<sup>+</sup>. A net ionization rate of 1 cm<sup>-3</sup> s<sup>-1</sup> produces good agreement between the model and INMS measurements of ion density. An ionization rate of 1 cm<sup>-3</sup> s<sup>-1</sup> implies a suprathermal electron flux of 1.2 × 10<sup>6</sup> cm<sup>-2</sup> s<sup>-1</sup> for an electron energy of 100 eV, a mean electron impact cross section of 4 × 10<sup>-16</sup> cm<sup>2</sup>, and a neutral density of 2 × 10<sup>9</sup> cm<sup>-3</sup>. This corresponds to an energy flux of 2 × 10<sup>-3</sup> erg cm<sup>-2</sup> s<sup>-1</sup>, which is of the order of a factor of ten less than the sub-solar EUV energy flux.

#### 2.4. Reaction list

The reaction list describes ion–molecule and ion–electron recombination reactions for ion species containing carbon, nitrogen and hydrogen. In a specific run, some oxygen-bearing ions (H<sub>2</sub>O<sup>+</sup>, H<sub>3</sub>O<sup>+</sup>, CH<sub>3</sub>OH<sub>2</sub><sup>+</sup>, CH<sub>3</sub>CHOH<sup>+</sup>) are considered as well. We do not distinguish the different isomers for these ions, except for C<sub>3</sub>H<sub>3</sub><sup>+</sup> (see Section 3.1).

Ion–molecule reactions are mostly retrieved from existing compilations of experimental data (Anicich and McEwan, 1997; Anicich et al., 2006; McEwan and Anicich, 2007) and from recently-published articles. A few reactions are obtained from databases dedicated to the interstellar medium (UMIST 2006; OSU 2007). Rates and products for most of the hydrocarbon ions can be considered as well described by the reaction list. However, the reactivity of most N-bearing ions and some heavier hydrocarbon ions is not available and we have to estimate their major production and loss pathways, based on chemical arguments. For those ions whose associated neutrals have a high PA, we assume that the 3 most abundant ions (HCNH<sup>+</sup>, CH<sub>5</sub><sup>+</sup>, C<sub>2</sub>H<sub>5</sub><sup>+</sup>) exchange a proton with the neutral at a rate of 3 × 10<sup>-9</sup> cm<sup>3</sup> s<sup>-1</sup>. Ion–electron recombination rates are retrieved from the literature. When the electron temperature dependence has not been determined, we assume the rate constant to be proportional to T<sub>e</sub><sup>-0.7</sup> and when no data is available, we estimate the recombination rate to be equal to 7 × 10<sup>-7</sup> (300/T<sub>e</sub>)<sup>0.7</sup> cm<sup>3</sup> s<sup>-1</sup>. The reaction list thus constructed includes ~150 ions containing up to 9 heavy atoms (carbon and nitrogen). The ~1250 reactions constituting the reaction list can be found as Supplementary material.

### 3. Results

The composition of Titan's ionosphere is governed by the flow of ionization to the constituents with the highest proton affinity. Thus, neutral species have a strong, even controlling, effect on the ion composition and the existence of many ions can only be understood as the consequence of significant density of associated neutrals. The mole fractions of 19 neutrals inferred from the measured densities of the ions, our ionization rate and reaction list are given in Table 1. The calculated densities of ions are given in Table 2 and the model spectrum is compared to the INMS spectrum in Fig. 2.

For many ions, production occurs through proton exchange reactions of the neutral with the abundant ions and loss occurs

Table 2  
Calculated densities of ions ( $\text{cm}^{-3}$ )

$m/z$	Species	Density ( $\text{cm}^{-3}$ )	Species	Density ( $\text{cm}^{-3}$ )	Species	Density ( $\text{cm}^{-3}$ )
12	$\text{C}^+$	$1.4 \times 10^{-2}$				
13	$\text{CH}^+$	$2.9 \times 10^{-2}$				
14	$\text{N}^+$	$2.8 \times 10^0$	$\text{CH}_2^+$	$6.6 \times 10^{-1}$		
15	$\text{CH}_3^+$	$9.5 \times 10^0$	$\text{NH}^+$	$8.7 \times 10^{-3}$		
16	$\text{CH}_4^+$	$6.8 \times 10^{-1}$	$\text{NH}_2^+$	$3.1 \times 10^{-3}$		
17	$\text{CH}_5^+$	$3.0 \times 10^1$	$\text{NH}_3^+$	$1.3 \times 10^{-2}$		
18	$\text{NH}_4^+$	$1.5 \times 10^1$				
25	$\text{C}_2\text{H}^+$	$5.7 \times 10^{-5}$				
26	$\text{C}_2\text{H}_2^+$	$2.7 \times 10^{-1}$	$\text{CN}^+$	$2.6 \times 10^{-4}$		
27	$\text{C}_2\text{H}_3^+$	$5.0 \times 10^0$	$\text{HCN}^+$	$2.9 \times 10^{-1}$		
28	$\text{HCNH}^+$	$4.6 \times 10^2$	$\text{C}_2\text{H}_4^+$	$1.3 \times 10^1$	$\text{N}_2^+$	$9.3 \times 10^0$
29	$\text{C}_2\text{H}_5^+$	$2.0 \times 10^2$	$\text{N}_2\text{H}^+$	$3.6 \times 10^0$	$\text{CH}_2\text{NH}^+$	$1.1 \times 10^{-2}$
30	$\text{CH}_2\text{NH}_2^+$	$4.8 \times 10^1$	$\text{C}_2\text{H}_6^+$	$7.1 \times 10^{-7}$		
31	$\text{C}_2\text{H}_7^+$	$4.8 \times 10^0$	$\text{CH}_3\text{NH}_2^+$	$1.9 \times 10^{-3}$		
36	$\text{C}_3^+$	$8.8 \times 10^{-4}$				
37	$\text{C}_3\text{H}^+$	$1.2 \times 10^{-2}$				
38	$\text{CNC}^+$	$3.1 \times 10^{-1}$	$\text{C}_3\text{H}_2^+$	$1.6 \times 10^{-3}$		
39	$\text{c-C}_3\text{H}_3^+$	$3.4 \times 10^1$	$\text{HC}_2\text{N}^+$	$3.1 \times 10^0$	$\text{l-C}_3\text{H}_3^+$	$1.8 \times 10^0$
40	$\text{HC}_2\text{NH}^+$	$2.3 \times 10^0$	$\text{C}_3\text{H}_4^+$	$9.3 \times 10^{-1}$		
41	$\text{C}_3\text{H}_5^+$	$1.0 \times 10^2$	$\text{CH}_3\text{CN}^+$	$3.2 \times 10^{-1}$		
42	$\text{CH}_3\text{CNH}^+$	$7.3 \times 10^1$	$\text{C}_3\text{H}_6^+$	$9.6 \times 10^{-2}$		
43	$\text{C}_3\text{H}_7^+$	$1.2 \times 10^0$	$\text{C}_2\text{H}_3\text{NH}_2^+$	$6.8 \times 10^{-3}$		
44	$\text{C}_3\text{H}_8^+$	$3.2 \times 10^{-4}$				
45	$\text{C}_3\text{H}_9^+$	$8.2 \times 10^{-2}$				
49	$\text{C}_4\text{H}^+$	$7.5 \times 10^{-5}$				
50	$\text{C}_4\text{H}_2^+$	$1.3 \times 10^0$	$\text{C}_3\text{N}^+$	$5.3 \times 10^{-5}$		
51	$\text{C}_4\text{H}_3^+$	$3.4 \times 10^1$	$\text{HC}_3\text{N}^+$	$6.7 \times 10^{-2}$		
52	$\text{HC}_3\text{NH}^+$	$1.4 \times 10^2$	$\text{C}_4\text{H}_4^+$	$2.8 \times 10^0$	$\text{C}_2\text{N}_2^+$	$1.4 \times 10^{-2}$
53	$\text{C}_4\text{H}_5^+$	$1.6 \times 10^1$	$\text{HC}_2\text{N}_2^+$	$7.7 \times 10^{-1}$	$\text{C}_2\text{H}_3\text{CN}^+$	$8.1 \times 10^{-2}$
54	$\text{C}_2\text{H}_3\text{CNH}^+$	$1.3 \times 10^2$	$\text{C}_4\text{H}_6^+$	$2.6 \times 10^{-3}$		
55	$\text{C}_4\text{H}_7^+$	$2.3 \times 10^0$	$\text{C}_2\text{H}_5\text{CN}^+$	$6.8 \times 10^{-6}$		
56	$\text{C}_2\text{H}_5\text{CNH}^+$	$5.1 \times 10^0$	$\text{C}_4\text{H}_8^+$	$1.4 \times 10^{-4}$		
57	$\text{C}_4\text{H}_9^+$	$2.7 \times 10^0$				
61	$\text{C}_5\text{H}^+$	$8.0 \times 10^{-4}$				
62	$\text{C}_4\text{N}^+$	$3.2 \times 10^{-3}$	$\text{C}_5\text{H}_2^+$	$1.0 \times 10^{-4}$		
63	$\text{C}_5\text{H}_3^+$	$2.6 \times 10^{-1}$	$\text{HC}_4\text{N}^+$	$1.9 \times 10^{-4}$		
64	$\text{C}_5\text{H}_4^+$	$2.5 \times 10^{-2}$	$\text{HC}_4\text{NH}^+$	$3.0 \times 10^{-4}$		
65	$\text{C}_5\text{H}_5^+$	$2.7 \times 10^1$	$\text{C}_4\text{H}_3\text{N}^+$	$2.9 \times 10^{-4}$		
66	$\text{C}_4\text{H}_3\text{NH}^+$	$3.9 \times 10^1$				
67	$\text{C}_5\text{H}_7^+$	$3.5 \times 10^1$	$\text{C}_4\text{H}_5\text{N}^+$	$3.3 \times 10^{-3}$		
68	$\text{C}_4\text{H}_5\text{NH}^+$	$4.7 \times 10^0$				
69	$\text{C}_5\text{H}_9^+$	$1.3 \times 10^1$				
73	$\text{C}_6\text{H}^+$	$1.4 \times 10^{-2}$				
74	$\text{C}_6\text{H}_2^+$	$6.5 \times 10^{-4}$	$\text{C}_5\text{N}^+$	$4.0 \times 10^{-7}$		
75	$\text{C}_6\text{H}_3^+$	$3.9 \times 10^0$	$\text{HC}_5\text{N}^+$	$5.8 \times 10^{-4}$		
76	$\text{HC}_5\text{NH}^+$	$9.7 \times 10^0$	$\text{C}_6\text{H}_4^+$	$5.2 \times 10^{-1}$		
77	$\text{C}_6\text{H}_5^+$	$2.7 \times 10^0$	$\text{C}_5\text{H}_3\text{N}^+$	$8.6 \times 10^{-1}$		
78	$\text{C}_5\text{H}_3\text{NH}^+$	$1.2 \times 10^0$	$\text{C}_6\text{H}_6^+$	$5.9 \times 10^{-2}$		
79	$\text{C}_6\text{H}_7^+$	$1.4 \times 10^1$	$\text{C}_5\text{H}_5\text{N}^+$	$8.1 \times 10^{-3}$		
80	$\text{C}_5\text{H}_5\text{NH}^+$	$4.1 \times 10^0$				
84	$\text{C}_7^+$	$3.1 \times 10^{-5}$				
85	$\text{C}_7\text{H}^+$	$3.0 \times 10^{-5}$				
86	$\text{C}_7\text{H}_2^+$	$4.6 \times 10^{-7}$				
87	$\text{C}_7\text{H}_3^+$	$2.1 \times 10^{-2}$				
88	$\text{C}_7\text{H}_4^+$	$8.2 \times 10^{-3}$	$\text{HC}_6\text{NH}^+$	$2.9 \times 10^{-3}$		
89	$\text{C}_7\text{H}_5^+$	$2.3 \times 10^0$				
90	$\text{C}_6\text{H}_3\text{NH}^+$	$2.9 \times 10^0$				

Table 2 (continued)

$m/z$	Species	Density ( $\text{cm}^{-3}$ )	Species	Density ( $\text{cm}^{-3}$ )	Species	Density ( $\text{cm}^{-3}$ )
91	$\text{C}_7\text{H}_7^+$	$2.1 \times 10^1$				
92	$\text{C}_6\text{H}_5\text{NH}^+$	$2.3 \times 10^{-1}$				
93	$\text{C}_7\text{H}_9^+$	$8.4 \times 10^{-1}$	$\text{C}_6\text{H}_7\text{N}^+$	$2.4 \times 10^{-3}$		
94	$\text{C}_6\text{H}_7\text{NH}^+$	$9.6 \times 10^{-1}$				
97	$\text{C}_8\text{H}^+$	$8.1 \times 10^{-7}$				
98	$\text{C}_8\text{H}_2^+$	$4.0 \times 10^{-6}$	$\text{C}_7\text{N}^+$	$6.4 \times 10^{-8}$		
99	$\text{C}_8\text{H}_3^+$	$9.7 \times 10^{-1}$	$\text{HC}_7\text{N}^+$	$1.7 \times 10^{-6}$		

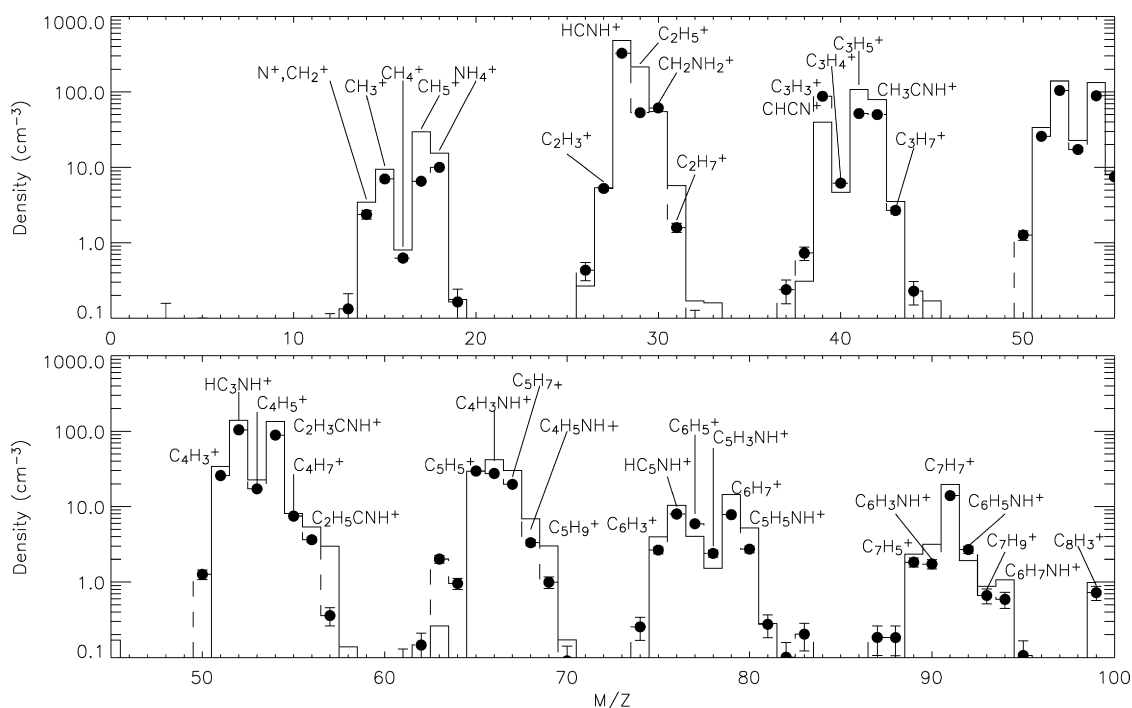


Fig. 2. INMS mass spectrum and model. The black dots show the INMS measurements, and the dashed line connects the points as in Fig. 1. The plain line represents the modeled spectrum with densities of selected neutral species tuned to reproduce the observations.

mostly through electron dissociative recombination. However, especially for the heavier ions, condensation reactions (reaction in which an ion and a molecule combine to form a larger ion with elimination of a small molecule) and radiative association reactions (reaction in which an ion and a molecule add to form a larger ion with emission of a photon) may also contribute to the production. In the following, we review the main production and loss pathways for those ions that are relevant to the density of neutrals. Their major production channels are illustrated in Fig. 3. We discuss the assumptions made in our model, and the reactions that need to be further studied in the laboratory.

### 3.1. Hydrocarbon ions

The primary ions produced by electron impact are  $\text{N}_2^+$ ,  $\text{N}^+$ ,  $\text{CH}_4^+$ ,  $\text{CH}_3^+$ ,  $\text{CH}_2^+$ ,  $\text{CH}^+$  and  $\text{C}^+$ . The principal production (reactions  $k_i$ ) and loss reactions (reactions  $k_i$  and  $\alpha_i$ ) of the main ions are listed in Tables 3 and 4, respectively.

$\text{CH}_5^+$  at  $m/z = 17$  ( $8 \text{ cm}^{-3}$  in the observed spectrum) is closely linked to the ionization of both  $\text{N}_2$  and  $\text{CH}_4$  through reactions  $k_1$  plus  $k_2$  and  $k_3$ , respectively. This ion is mostly lost

through reactions with  $\text{C}_2\text{H}_4$ ,  $\text{HCN}$  and  $\text{C}_2\text{H}_2$  ( $k_4$ – $k_6$ ), and electron dissociative recombination ( $\alpha_1$ ).

$\text{C}_2\text{H}_5^+$  at  $m/z = 29$  ( $50 \text{ cm}^{-3}$  in the observed spectrum) is closely linked to the ionization of  $\text{CH}_4$  through reactions  $k_7$  and  $k_2$ ,  $k_3$  plus  $k_8$ . This ion is mostly lost through electron dissociative recombination ( $\alpha_2$ ), and reactions with  $\text{HCN}$  and  $\text{C}_2\text{H}_4$  ( $k_9$ ,  $k_{10}$ ). Note that because  $\text{C}_2\text{H}_4$  has only a moderate PA, the major formation channel for  $\text{C}_2\text{H}_5^+$  is not a proton exchange reaction. Consequently, the abundance of  $\text{C}_2\text{H}_4$  cannot be inferred from the protonated molecule,  $\text{C}_2\text{H}_5^+$ , as is done for the other neutrals. However, it can be retrieved from  $\text{C}_3\text{H}_5^+$ .

$\text{C}_3\text{H}_5^+$  at  $m/z = 41$  ( $50 \text{ cm}^{-3}$  in the observed spectrum) is produced largely via reactions with  $\text{C}_2\text{H}_4$  and  $\text{CH}_4$  ( $k_{11}$ ,  $k_{12}$ ), and mostly lost through electron dissociative recombination ( $\alpha_3$ ). From reactions  $k_{11}$  and  $\alpha_3$ , a mole fraction of  $1.0 \times 10^{-3}$  for  $\text{C}_2\text{H}_4$  can be retrieved.

$\text{C}_3\text{H}_3^+$  is known to exist in two possible low-energy forms: the acyclic propargyl ion,  $1\text{-C}_3\text{H}_3^+$ , and the cyclopropenylum ion,  $c\text{-C}_3\text{H}_3^+$ , the latter being much less reactive than the former.  $\text{C}_3\text{H}_3^+$  is one of the most abundant ions in the spectrum ( $\sim 90 \text{ cm}^{-3}$ ) and while  $c\text{-C}_3\text{H}_3^+$  is exclusively lost by elec-

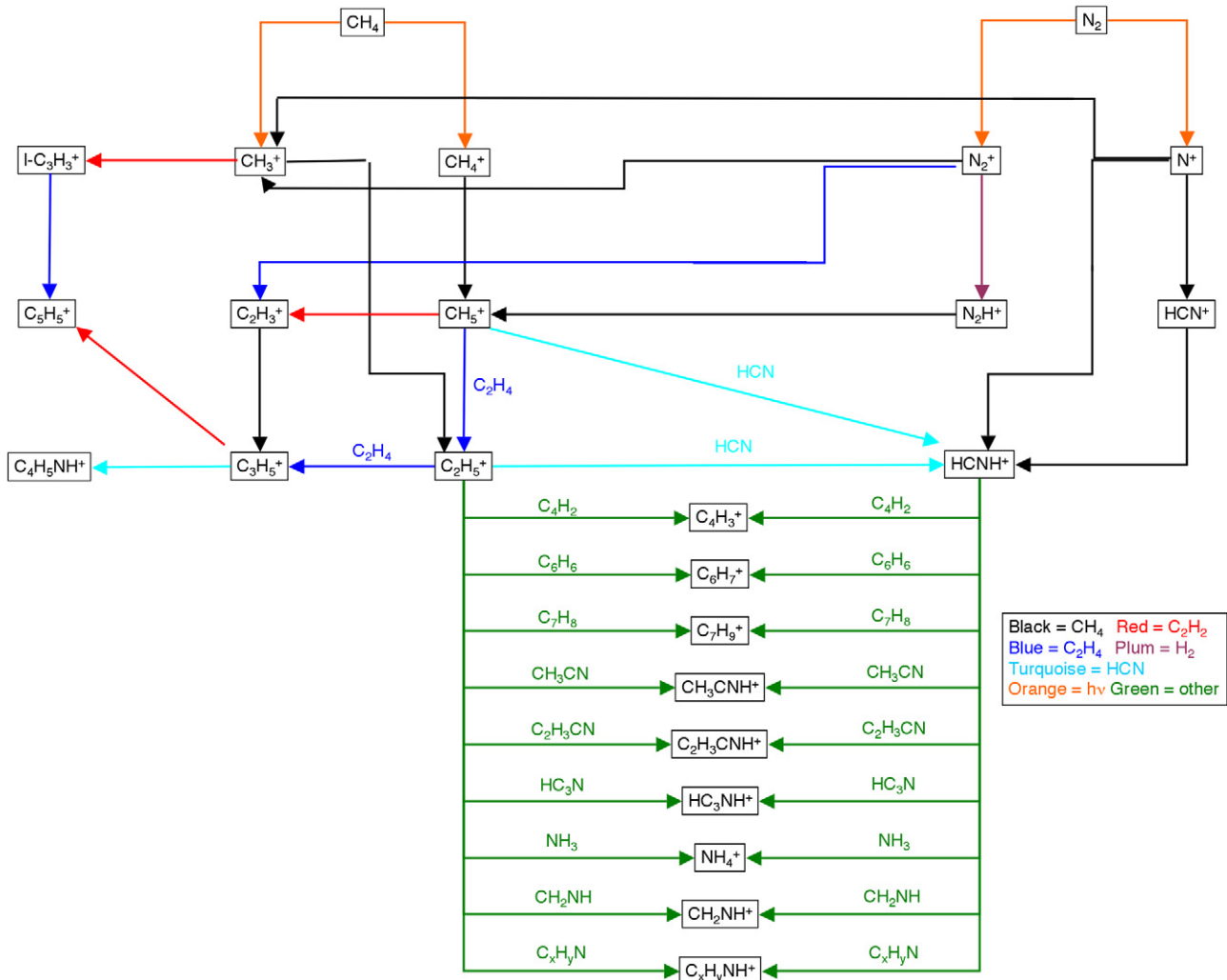


Fig. 3. Flowchart representing the major reactions used to determine the neutral densities.

tron recombination ( $\alpha_4$ ),  $l\text{-C}_3\text{H}_3^+$  can react to form heavier ions ( $k_{13}$ ,  $k_{14}$ ). It is consequently important to distinguish these 2 species when trying to fit the INMS spectrum. The major sources of  $\text{C}_3\text{H}_3^+$  ( $m/z = 39$ ) in our model are via the reactions of various ions with  $\text{C}_2\text{H}_2$  ( $k_{15}$ – $k_{17}$ ). The conformation of the  $\text{C}_3\text{H}_3^+$  product was not established for these reactions. We tried to determine an approximate ratio of  $l\text{-C}_3\text{H}_3^+/c\text{-C}_3\text{H}_3^+$  by making measurements using Selected Ion Flow Tube Mass Spectrometry (SIFT-MS). A titration reaction using  $\text{C}_2\text{H}_2$  or  $\text{C}_2\text{H}_4$  as the titrant allowed an estimate of the isomeric ratio to be found.  $l\text{-C}_3\text{H}_3^+$  is reactive with the titrant but  $c\text{-C}_3\text{H}_3^+$  is not. It was found that the first reaction gives  $\sim 75\%$  of  $l\text{-C}_3\text{H}_3^+$  while its yield in the third reaction is  $< 10\%$  (Edwards et al., in preparation). Because of its low rate constant, the amount of  $\text{C}_3\text{H}_3^+$  produced in the second reaction was insufficient to allow a determination of the isomeric ratio. This leaves us with a lower limit for the ratio of  $l\text{-C}_3\text{H}_3^+/c\text{-C}_3\text{H}_3^+$  of 20%. Our model underestimates the density at  $m/z = 39$  by a factor of 3.  $c\text{-C}_3\text{H}_3^+$  being much less reactive than  $l\text{-C}_3\text{H}_3^+$ , it contributes to most of the signal at  $m/z = 39$  and decreasing the  $l\text{-C}_3\text{H}_3^+/c\text{-C}_3\text{H}_3^+$  would increase the density at  $m/z = 39$ . However, even if all  $\text{C}_3\text{H}_3^+$  has the  $c\text{-C}_3\text{H}_3^+$  structure, the den-

sity at  $m/z = 39$  increases by 25% only. Note that a factor of 3 is within the error bars induced by uncertainties in the reaction rates and quantum yields (Carrasco et al., 2007).

We identify  $m/z = 51$  as  $\text{C}_4\text{H}_3^+$  ( $30 \text{ cm}^{-3}$  in the observed spectrum). This ion, first mentioned in Fox and Yelle (1997), is mostly produced in our model from proton exchange reactions ( $k_{18}$ ,  $k_{19}$ ). Condensation and radiative association reactions are negligible ( $\sim 3\%$ ).  $\text{C}_4\text{H}_3^+$  is lost through electron dissociative recombination ( $\alpha_5$ ) and reaction with  $\text{C}_2\text{H}_4$  and  $\text{C}_2\text{H}_2$  ( $k_{20}$ ,  $k_{21}$ ). A  $\text{C}_4\text{H}_2$  mole fraction of  $1 \times 10^{-5}$  is determined from the density of  $\text{C}_4\text{H}_3^+$ .

The density of  $\text{C}_5\text{H}_5^+$  at  $m/z = 65$  ( $30 \text{ cm}^{-3}$  in the observed spectrum) is well reproduced in the model via two condensation reactions ( $k_{22}$ ,  $k_{23}$ ) and loss through electron dissociative recombination ( $\alpha_6$ ). It follows that proton transfer reactions from protonated neutrals with low PA to  $\text{C}_5\text{H}_4$  have to be negligible for the model not to overestimate the ion densities. We can then retrieve an upper limit of  $10^{-6}$  for the mole fraction of  $\text{C}_5\text{H}_4$ .

The ion at  $m/z = 75$  ( $3 \text{ cm}^{-3}$  in the observed spectrum),  $\text{C}_6\text{H}_3^+$ , has not been predicted to be present in Titan's ionosphere. It is almost exclusively produced in our model from proton exchange reactions with  $\text{C}_6\text{H}_2$  ( $k_{24}$ ,  $k_{25}$ ) and lost

Table 3

Principal production reactions for the main ions. The third column indicates the contribution (%) of each reaction to the total production of the corresponding ion as inferred by the model. Only reactions contributing to more than ~10% or discussed in the text are presented. Rate constants in italic are estimated

Species	Reactions	$k$ (cm <sup>3</sup> s <sup>-1</sup> )	%	R#
CH <sub>5</sub> <sup>+</sup>	N <sub>2</sub> <sup>+</sup> + H <sub>2</sub> → N <sub>2</sub> H <sup>+</sup> + H	2.0 × 10 <sup>-9</sup>	–	k <sub>1</sub>
	N <sub>2</sub> H <sup>+</sup> + CH <sub>4</sub> → CH <sub>5</sub> <sup>+</sup> + N <sub>2</sub>	8.9 × 10 <sup>-10</sup>	80	k <sub>2</sub>
	CH <sub>4</sub> <sup>+</sup> + CH <sub>4</sub> → CH <sub>5</sub> <sup>+</sup> + CH <sub>3</sub>	1.1 × 10 <sup>-9</sup>	20	k <sub>3</sub>
C <sub>2</sub> H <sub>5</sub> <sup>+</sup>	CH <sub>3</sub> <sup>+</sup> + CH <sub>4</sub> → C <sub>2</sub> H <sub>5</sub> <sup>+</sup> + H <sub>2</sub>	1.1 × 10 <sup>-9</sup>	82	k <sub>7</sub>
	CH <sub>5</sub> <sup>+</sup> + C <sub>2</sub> H <sub>4</sub> → C <sub>2</sub> H <sub>5</sub> <sup>+</sup> + CH <sub>4</sub>	1.5 × 10 <sup>-9</sup>	13	k <sub>8</sub>
c,l-C <sub>3</sub> H <sub>3</sub> <sup>+</sup>	CH <sub>3</sub> <sup>+</sup> + C <sub>2</sub> H <sub>2</sub> → c,l-C <sub>3</sub> H <sub>3</sub> <sup>+</sup> + H <sub>2</sub>	2.9 × 10 <sup>-10</sup>	34	k <sub>15</sub>
	C <sub>2</sub> H <sub>5</sub> <sup>+</sup> + C <sub>2</sub> H <sub>2</sub> → c,l-C <sub>3</sub> H <sub>3</sub> <sup>+</sup> + CH <sub>4</sub>	6.8 × 10 <sup>-11</sup>	33	k <sub>16</sub>
	C <sub>2</sub> H <sub>4</sub> <sup>+</sup> + C <sub>2</sub> H <sub>2</sub> → c,l-C <sub>3</sub> H <sub>3</sub> <sup>+</sup> + CH <sub>3</sub>	6.5 × 10 <sup>-10</sup>	21	k <sub>17</sub>
C <sub>3</sub> H <sub>5</sub> <sup>+</sup>	C <sub>2</sub> H <sub>5</sub> <sup>+</sup> + C <sub>2</sub> H <sub>4</sub> → C <sub>3</sub> H <sub>5</sub> <sup>+</sup> + CH <sub>4</sub>	3.6 × 10 <sup>-10</sup>	60	k <sub>11</sub>
	C <sub>2</sub> H <sub>3</sub> <sup>+</sup> + CH <sub>4</sub> → C <sub>3</sub> H <sub>5</sub> <sup>+</sup> + H <sub>2</sub>	1.9 × 10 <sup>-10</sup>	22	k <sub>12</sub>
C <sub>4</sub> H <sub>3</sub> <sup>+</sup>	HCNH <sup>+</sup> + C <sub>4</sub> H <sub>2</sub> → C <sub>4</sub> H <sub>3</sub> <sup>+</sup> + HCN	1.8 × 10 <sup>-9</sup>	52	k <sub>18</sub>
	C <sub>2</sub> H <sub>5</sub> <sup>+</sup> + C <sub>4</sub> H <sub>2</sub> → C <sub>4</sub> H <sub>3</sub> <sup>+</sup> + C <sub>2</sub> H <sub>4</sub>	3.0 × 10 <sup>-9</sup>	39	k <sub>19</sub>
C <sub>5</sub> H <sub>5</sub> <sup>+</sup>	C <sub>3</sub> H <sub>5</sub> <sup>+</sup> + C <sub>2</sub> H <sub>2</sub> → C <sub>5</sub> H <sub>5</sub> <sup>+</sup> + H <sub>2</sub>	3.8 × 10 <sup>-10</sup>	87	k <sub>22</sub>
	l-C <sub>3</sub> H <sub>3</sub> <sup>+</sup> + C <sub>2</sub> H <sub>4</sub> → C <sub>5</sub> H <sub>5</sub> <sup>+</sup> + H <sub>2</sub>	5.5 × 10 <sup>-10</sup>	9	k <sub>23</sub>
C <sub>6</sub> H <sub>3</sub> <sup>+</sup>	HCNH <sup>+</sup> + C <sub>6</sub> H <sub>2</sub> → C <sub>6</sub> H <sub>3</sub> <sup>+</sup> + HCN	3.0 × 10 <sup>-9</sup>	57	k <sub>24</sub>
	C <sub>2</sub> H <sub>5</sub> <sup>+</sup> + C <sub>6</sub> H <sub>2</sub> → C <sub>6</sub> H <sub>3</sub> <sup>+</sup> + C <sub>2</sub> H <sub>4</sub>	3.0 × 10 <sup>-9</sup>	26	k <sub>25</sub>
	C <sub>4</sub> H <sub>3</sub> <sup>+</sup> + C <sub>4</sub> H <sub>2</sub> → C <sub>6</sub> H <sub>3</sub> <sup>+</sup> + C <sub>2</sub> H <sub>2</sub>	7.4 × 10 <sup>-10</sup>	12	k <sub>27</sub>
C <sub>6</sub> H <sub>7</sub> <sup>+</sup>	HCNH <sup>+</sup> + C <sub>6</sub> H <sub>6</sub> → C <sub>6</sub> H <sub>7</sub> <sup>+</sup> + HCN	3.0 × 10 <sup>-9</sup>	49	k <sub>28</sub>
	C <sub>2</sub> H <sub>5</sub> <sup>+</sup> + C <sub>6</sub> H <sub>6</sub> → C <sub>6</sub> H <sub>7</sub> <sup>+</sup> + C <sub>2</sub> H <sub>4</sub>	3.0 × 10 <sup>-9</sup>	22	k <sub>29</sub>
	C <sub>4</sub> H <sub>5</sub> <sup>+</sup> + C <sub>2</sub> H <sub>4</sub> → C <sub>6</sub> H <sub>7</sub> <sup>+</sup> + H <sub>2</sub>	6.3 × 10 <sup>-11</sup>	13	k <sub>30</sub>
C <sub>7</sub> H <sub>5</sub> <sup>+</sup>	HCNH <sup>+</sup> + C <sub>7</sub> H <sub>4</sub> → C <sub>7</sub> H <sub>5</sub> <sup>+</sup> + HCN	3.0 × 10 <sup>-9</sup>	59	k <sub>31</sub>
	C <sub>2</sub> H <sub>5</sub> <sup>+</sup> + C <sub>7</sub> H <sub>4</sub> → C <sub>7</sub> H <sub>5</sub> <sup>+</sup> + C <sub>2</sub> H <sub>4</sub>	3.0 × 10 <sup>-9</sup>	27	k <sub>32</sub>
	C <sub>5</sub> H <sub>5</sub> <sup>+</sup> + C <sub>4</sub> H <sub>2</sub> → C <sub>7</sub> H <sub>5</sub> <sup>+</sup> + C <sub>2</sub> H <sub>2</sub>	2.2 × 10 <sup>-10</sup>	7	k <sub>33</sub>
C <sub>7</sub> H <sub>9</sub> <sup>+</sup>	HCNH <sup>+</sup> + C <sub>7</sub> H <sub>8</sub> → C <sub>7</sub> H <sub>9</sub> <sup>+</sup> + HCN	3.0 × 10 <sup>-9</sup>	65	k <sub>34</sub>
	C <sub>2</sub> H <sub>5</sub> <sup>+</sup> + C <sub>7</sub> H <sub>8</sub> → C <sub>7</sub> H <sub>9</sub> <sup>+</sup> + C <sub>2</sub> H <sub>4</sub>	3.0 × 10 <sup>-9</sup>	29	k <sub>35</sub>
C <sub>8</sub> H <sub>3</sub> <sup>+</sup>	HCNH <sup>+</sup> + C <sub>8</sub> H <sub>2</sub> → C <sub>8</sub> H <sub>3</sub> <sup>+</sup> + HCN	3.0 × 10 <sup>-9</sup>	66	k <sub>36</sub>
	C <sub>2</sub> H <sub>5</sub> <sup>+</sup> + C <sub>8</sub> H <sub>2</sub> → C <sub>8</sub> H <sub>3</sub> <sup>+</sup> + C <sub>2</sub> H <sub>4</sub>	3.0 × 10 <sup>-9</sup>	30	k <sub>37</sub>
	C <sub>4</sub> H <sub>3</sub> <sup>+</sup> + C <sub>6</sub> H <sub>2</sub> → C <sub>8</sub> H <sub>3</sub> <sup>+</sup> + C <sub>2</sub> H <sub>2</sub>	~7.4 × 10 <sup>-10</sup>	4	k <sub>38</sub>
NH <sub>4</sub> <sup>+</sup>	HCNH <sup>+</sup> + NH <sub>3</sub> → NH <sub>4</sub> <sup>+</sup> + HCN	2.3 × 10 <sup>-9</sup>	47	k <sub>39</sub>
	C <sub>2</sub> H <sub>5</sub> <sup>+</sup> + NH <sub>3</sub> → NH <sub>4</sub> <sup>+</sup> + C <sub>2</sub> H <sub>4</sub>	2.1 × 10 <sup>-9</sup>	19	k <sub>40</sub>
HCNH <sup>+</sup>	C <sub>2</sub> H <sub>5</sub> <sup>+</sup> + HCN → HCNH <sup>+</sup> + C <sub>2</sub> H <sub>4</sub>	2.7 × 10 <sup>-9</sup>	61	k <sub>42</sub>
	N <sup>+</sup> + CH <sub>4</sub> → HCNH <sup>+</sup> + H <sub>2</sub>	4.1 × 10 <sup>-10</sup>	18	k <sub>43</sub>
	CH <sub>5</sub> <sup>+</sup> + HCN → HCNH <sup>+</sup> + CH <sub>4</sub>	3.0 × 10 <sup>-9</sup>	10	k <sub>41</sub>
	HCN <sup>+</sup> + CH <sub>4</sub> → HCNH <sup>+</sup> + CH <sub>3</sub>	1.1 × 10 <sup>-9</sup>	5	k <sub>44</sub>
CH <sub>2</sub> NH <sub>2</sub> <sup>+</sup>	HCNH <sup>+</sup> + CH <sub>2</sub> NH → CH <sub>2</sub> NH <sub>2</sub> <sup>+</sup> + HCN	3.0 × 10 <sup>-9</sup>	65	k <sub>50</sub>
	C <sub>2</sub> H <sub>5</sub> <sup>+</sup> + CH <sub>2</sub> NH → CH <sub>2</sub> NH <sub>2</sub> <sup>+</sup> + C <sub>2</sub> H <sub>4</sub>	3.0 × 10 <sup>-9</sup>	30	k <sub>51</sub>
	CH <sub>3</sub> <sup>+</sup> + NH <sub>3</sub> → CH <sub>2</sub> NH <sub>2</sub> <sup>+</sup> + H <sub>2</sub>	1.5 × 10 <sup>-9</sup>	1	k <sub>47</sub>
	CH <sub>3</sub> <sup>+</sup> + CH <sub>3</sub> NH <sub>2</sub> → CH <sub>2</sub> NH <sub>2</sub> <sup>+</sup> + CH <sub>4</sub>	1.4 × 10 <sup>-9</sup>	<0.002	k <sub>48</sub>
	N <sub>2</sub> <sup>+</sup> + CH <sub>3</sub> NH <sub>2</sub> → CH <sub>2</sub> NH <sub>2</sub> <sup>+</sup> + N <sub>2</sub> + H	8.8 × 10 <sup>-10</sup>	<0.001	k <sub>49</sub>
CH <sub>3</sub> CNH <sup>+</sup>	HCNH <sup>+</sup> + CH <sub>3</sub> CN → CH <sub>3</sub> CNH <sup>+</sup> + HCN	3.8 × 10 <sup>-9</sup>	50	k <sub>52</sub>
	C <sub>2</sub> H <sub>5</sub> <sup>+</sup> + CH <sub>3</sub> CN → CH <sub>3</sub> CNH <sup>+</sup> + C <sub>2</sub> H <sub>4</sub>	3.8 × 10 <sup>-9</sup>	22	k <sub>53</sub>
HC <sub>3</sub> NH <sup>+</sup>	HCNH <sup>+</sup> + HC <sub>3</sub> N → HC <sub>3</sub> NH <sup>+</sup> + HCN	3.4 × 10 <sup>-9</sup>	61	k <sub>54</sub>
	C <sub>2</sub> H <sub>5</sub> <sup>+</sup> + HC <sub>3</sub> N → HC <sub>3</sub> NH <sup>+</sup> + C <sub>2</sub> H <sub>4</sub>	3.6 × 10 <sup>-9</sup>	29	k <sub>55</sub>
C <sub>2</sub> H <sub>3</sub> CNH <sup>+</sup>	HCNH <sup>+</sup> + C <sub>2</sub> H <sub>3</sub> CN → C <sub>2</sub> H <sub>3</sub> CNH <sup>+</sup> + HCN	4.5 × 10 <sup>-9</sup>	71	k <sub>56</sub>
	C <sub>2</sub> H <sub>5</sub> <sup>+</sup> + C <sub>2</sub> H <sub>3</sub> CN → C <sub>2</sub> H <sub>3</sub> CNH <sup>+</sup> + C <sub>2</sub> H <sub>4</sub>	3.0 × 10 <sup>-9</sup>	21	k <sub>57</sub>
C <sub>2</sub> H <sub>5</sub> CNH <sup>+</sup>	HCNH <sup>+</sup> + C <sub>2</sub> H <sub>5</sub> CN → C <sub>2</sub> H <sub>5</sub> CNH <sup>+</sup> + HCN	3.0 × 10 <sup>-9</sup>	66	k <sub>59</sub>
	C <sub>2</sub> H <sub>5</sub> <sup>+</sup> + C <sub>2</sub> H <sub>5</sub> CN → C <sub>2</sub> H <sub>5</sub> CNH <sup>+</sup> + C <sub>2</sub> H <sub>4</sub>	3.0 × 10 <sup>-9</sup>	30	k <sub>60</sub>
	CH <sub>3</sub> <sup>+</sup> + CH <sub>3</sub> CN → C <sub>2</sub> H <sub>5</sub> CNH <sup>+</sup> + <i>hν</i>	9.0 × 10 <sup>-11</sup>	0.25	k <sub>58</sub>

(continued on next page)

Table 3 (continued)

Species	Reactions	$k$ (cm <sup>3</sup> s <sup>-1</sup> )	%	R#
C <sub>4</sub> H <sub>3</sub> NH <sup>+</sup>	I-C <sub>3</sub> H <sub>3</sub> <sup>+</sup> + HCN → C <sub>4</sub> H <sub>3</sub> NH <sup>+</sup> + $h\nu$	$4.8 \times 10^{-10}$	~20	k <sub>61</sub>
	HCNH <sup>+</sup> + C <sub>4</sub> H <sub>3</sub> N → C <sub>4</sub> H <sub>3</sub> NH <sup>+</sup> + HCN	$3.0 \times 10^{-9}$	52	k <sub>62</sub>
	C <sub>2</sub> H <sub>5</sub> <sup>+</sup> + C <sub>4</sub> H <sub>3</sub> N → C <sub>4</sub> H <sub>3</sub> NH <sup>+</sup> + C <sub>2</sub> H <sub>4</sub>	$3.0 \times 10^{-9}$	23	k <sub>63</sub>
C <sub>4</sub> H <sub>5</sub> NH <sup>+</sup>	C <sub>3</sub> H <sub>5</sub> <sup>+</sup> + HCN → C <sub>4</sub> H <sub>5</sub> NH <sup>+</sup> + $h\nu$	$5.0 \times 10^{-11}$	99	k <sub>64</sub>
	HC <sub>3</sub> NH <sup>+</sup> + C <sub>2</sub> H <sub>4</sub> → C <sub>4</sub> H <sub>5</sub> NH <sup>+</sup> + H	$<1.3 \times 10^{-9}$	–	k <sub>65</sub>
C <sub>x</sub> H <sub>y</sub> NH <sup>+</sup>	HCNH <sup>+</sup> + C <sub>x</sub> H <sub>y</sub> N → C <sub>x</sub> H <sub>y</sub> NH <sup>+</sup> + HCN	$3.0 \times 10^{-9}$	~66	k <sub>66</sub>
	C <sub>2</sub> H <sub>5</sub> <sup>+</sup> + C <sub>x</sub> H <sub>y</sub> N → C <sub>x</sub> H <sub>y</sub> NH <sup>+</sup> + C <sub>2</sub> H <sub>4</sub>	$3.0 \times 10^{-9}$	~30	k <sub>67</sub>
CH <sub>3</sub> NH <sub>3</sub> <sup>+</sup>	HCNH <sup>+</sup> + CH <sub>3</sub> NH <sub>2</sub> → CH <sub>3</sub> NH <sub>3</sub> <sup>+</sup> + HCN	$3.0 \times 10^{-9}$	74	k <sub>68</sub>
	C <sub>2</sub> H <sub>5</sub> <sup>+</sup> + CH <sub>3</sub> NH <sub>2</sub> → CH <sub>3</sub> NH <sub>3</sub> <sup>+</sup> + C <sub>2</sub> H <sub>4</sub>	$1.9 \times 10^{-9}$	21	k <sub>69</sub>
N <sub>2</sub> H <sub>5</sub> <sup>+</sup>	HCNH <sup>+</sup> + N <sub>2</sub> H <sub>4</sub> → N <sub>2</sub> H <sub>5</sub> <sup>+</sup> + HCN	$3.0 \times 10^{-9}$	66	k <sub>70</sub>
	C <sub>2</sub> H <sub>5</sub> <sup>+</sup> + N <sub>2</sub> H <sub>4</sub> → N <sub>2</sub> H <sub>5</sub> <sup>+</sup> + C <sub>2</sub> H <sub>4</sub>	$3.0 \times 10^{-9}$	30	k <sub>71</sub>
H <sub>3</sub> O <sup>+</sup>	C <sub>2</sub> H <sub>5</sub> <sup>+</sup> + H <sub>2</sub> O → H <sub>3</sub> O <sup>+</sup> + C <sub>2</sub> H <sub>4</sub>	$1.9 \times 10^{-9}$	71	k <sub>72</sub>
	CH <sub>5</sub> <sup>+</sup> + H <sub>2</sub> O → H <sub>3</sub> O <sup>+</sup> + CH <sub>4</sub>	$3.7 \times 10^{-9}$	21	k <sub>73</sub>
CH <sub>3</sub> OH <sub>2</sub> <sup>+</sup>	HCNH <sup>+</sup> + CH <sub>3</sub> OH → CH <sub>3</sub> OH <sub>2</sub> <sup>+</sup> + HCN	$3.0 \times 10^{-9}$	66	k <sub>74</sub>
	C <sub>2</sub> H <sub>5</sub> <sup>+</sup> + CH <sub>3</sub> OH → CH <sub>3</sub> OH <sub>2</sub> <sup>+</sup> + C <sub>2</sub> H <sub>4</sub>	$3.0 \times 10^{-9}$	30	k <sub>75</sub>
CH <sub>3</sub> CHOH <sup>+</sup>	HCNH <sup>+</sup> + CH <sub>3</sub> CHO → CH <sub>3</sub> CHOH <sup>+</sup> + HCN	$3.0 \times 10^{-9}$	66	k <sub>76</sub>
	C <sub>2</sub> H <sub>5</sub> <sup>+</sup> + CH <sub>3</sub> CHO → CH <sub>3</sub> CHOH <sup>+</sup> + C <sub>2</sub> H <sub>4</sub>	$3.4 \times 10^{-9}$	30	k <sub>77</sub>

through electron dissociative recombination ( $\alpha_7$ ) and reaction with C<sub>2</sub>H<sub>2</sub> (k<sub>26</sub>). The major condensation reaction producing C<sub>6</sub>H<sub>3</sub><sup>+</sup> (k<sub>27</sub>) for a measured C<sub>4</sub>H<sub>3</sub><sup>+</sup> density of 30 cm<sup>-3</sup> and a C<sub>4</sub>H<sub>2</sub> mole fraction of 10<sup>-5</sup>, would give a C<sub>6</sub>H<sub>3</sub><sup>+</sup> density of ~0.3 cm<sup>-3</sup>. This is a factor of 10 lower than observed; thus C<sub>6</sub>H<sub>3</sub><sup>+</sup> is produced primarily by proton exchange and the required C<sub>6</sub>H<sub>2</sub> mole fraction is 8 × 10<sup>-7</sup>.

C<sub>6</sub>H<sub>7</sub><sup>+</sup> at  $m/z = 79$  (8 cm<sup>-3</sup> in the observed spectrum) is mostly produced by proton exchange reactions (k<sub>28</sub>, k<sub>29</sub>) and from k<sub>30</sub> involving C<sub>2</sub>H<sub>4</sub>. It is lost almost entirely to electron dissociative recombination ( $\alpha_8$ ). Condensation and radiative association reactions, including k<sub>30</sub>, contribute to about 30% of the measured density at  $m/z = 79$ . We retrieve a mole fraction for C<sub>6</sub>H<sub>6</sub> of about 3 × 10<sup>-6</sup>. Note that the reaction between C<sub>5</sub>H<sub>5</sub><sup>+</sup> and C<sub>3</sub>H<sub>4</sub> suggested by Keller et al. (1998) as a main production channel for C<sub>6</sub>H<sub>7</sub><sup>+</sup> has recently been reinvestigated (Anicich et al., 2006). The reaction was found to be slow and an upper limit of 5.0 × 10<sup>-12</sup> cm<sup>3</sup> s<sup>-1</sup> was obtained. As a consequence, this process is a negligible source of C<sub>6</sub>H<sub>7</sub><sup>+</sup> in our model.

None of the previous models predicted C<sub>7</sub>H<sub>5</sub><sup>+</sup> at  $m/z = 89$  (8 cm<sup>-3</sup> in the observed spectrum). This ion is mostly formed via proton exchange reactions (k<sub>31</sub>, k<sub>32</sub>) and from the condensation reaction k<sub>33</sub> involving C<sub>4</sub>H<sub>2</sub>. It is lost almost entirely to electron dissociative recombination ( $\alpha_9$ ). With condensation reactions alone and a C<sub>4</sub>H<sub>2</sub> mole fraction of 10<sup>-5</sup>, our calculated density at  $m/z = 89$  would be a factor of 10 smaller than the observed density. We infer a mole fraction of C<sub>7</sub>H<sub>4</sub> of 3 × 10<sup>-7</sup>.

The situation is a bit more complicated for C<sub>7</sub>H<sub>9</sub><sup>+</sup> at  $m/z = 93$  (0.7 cm<sup>-3</sup> in the observed spectrum), because of the lack of chemical pathways to produce this ion. C<sub>7</sub>H<sub>9</sub><sup>+</sup> production rate from any exothermic condensation reaction, even if happening at the collisional rate, falls short by at least an order of magnitude. Proton exchange reactions of C<sub>7</sub>H<sub>8</sub> with abundant ions

seem to be the only process efficient enough to reproduce the C<sub>7</sub>H<sub>9</sub><sup>+</sup> density (k<sub>34</sub>, k<sub>35</sub>). We assume that this ion is mostly lost through electron dissociative recombination ( $\alpha_{10}$ ) and retrieve a C<sub>7</sub>H<sub>8</sub> mole fraction of 2 × 10<sup>-7</sup>.

Data on reactions forming C<sub>8</sub>H<sub>3</sub><sup>+</sup>, at  $m/z = 99$  are very scarce as well (0.8 cm<sup>-3</sup> in the observed spectrum). Similar condensation reactions as those forming C<sub>6</sub>H<sub>3</sub><sup>+</sup> should apply to C<sub>8</sub>H<sub>3</sub><sup>+</sup>, for example reaction k<sub>36</sub>. However, the analogous reaction could only account for 10% of the C<sub>6</sub>H<sub>3</sub><sup>+</sup> density. Similarly, k<sub>36</sub> implies a density for C<sub>8</sub>H<sub>3</sub><sup>+</sup> of 3 × 10<sup>-2</sup>, that is a factor of 25 lower than observed. Other possible reactions are even less efficient. Proton exchange reactions are again required to explain the density of C<sub>8</sub>H<sub>3</sub><sup>+</sup> (k<sub>37</sub>, k<sub>38</sub>). We assume that C<sub>8</sub>H<sub>3</sub><sup>+</sup> is mostly lost through electron recombination ( $\alpha_{11}$ ) and infer a mole fraction for C<sub>8</sub>H<sub>2</sub> of 2 × 10<sup>-7</sup>.

### 3.2. N-bearing species

NH<sub>4</sub><sup>+</sup> at  $m/z = 18$  (10 cm<sup>-3</sup> in the observed spectrum) is almost exclusively created by proton attachment to NH<sub>3</sub> as indicated by reactions k<sub>39</sub> and k<sub>40</sub> (Cravens et al., 2006) and lost through electron dissociative recombination ( $\alpha_{12}$ ). A mole fraction for NH<sub>3</sub> of 7 × 10<sup>-6</sup> is required to match the observed density of 10 cm<sup>-3</sup> at  $m/z = 18$ .

Proton exchange of C<sub>2</sub>H<sub>5</sub><sup>+</sup> and CH<sub>5</sub><sup>+</sup> with HCN (k<sub>41</sub>, k<sub>42</sub>) is responsible for ~70% of the HCNH<sup>+</sup> production at  $m/z = 28$  (300 cm<sup>-3</sup> in the observed spectrum). The remainder of the production is via various condensation reactions (k<sub>43</sub>, k<sub>44</sub>) in agreement with previous models (Banaszkiwicz et al., 2000; Fox and Yelle, 1997; Keller et al., 1998). Electron dissociative recombination ( $\alpha_{13}$ ) and proton exchange to HC<sub>3</sub>N and C<sub>2</sub>H<sub>3</sub>CN account for 80% of the loss of HCNH<sup>+</sup> (k<sub>45</sub>, k<sub>46</sub>). We retrieve a mole fraction of 2 × 10<sup>-4</sup> for HCN.

Table 4  
Principal loss reactions for the main ions. Electron dissociative recombination rates ( $\alpha$ ) are for an electron temperature of 718 K. Same as Table 3

Species	Reactions	$k/\alpha$ (cm <sup>3</sup> s <sup>-1</sup> )	%	R#
CH <sub>5</sub> <sup>+</sup>	CH <sub>5</sub> <sup>+</sup> + C <sub>2</sub> H <sub>4</sub> → C <sub>2</sub> H <sub>5</sub> <sup>+</sup> + CH <sub>4</sub>	1.5 × 10 <sup>-9</sup>	41	k <sub>4</sub>
	CH <sub>5</sub> <sup>+</sup> + HCN → HCNH <sup>+</sup> + CH <sub>4</sub>	3.0 × 10 <sup>-9</sup>	16	k <sub>5</sub>
	CH <sub>5</sub> <sup>+</sup> + e <sup>-</sup> → products	6.0 × 10 <sup>-7</sup>	14	$\alpha$ <sub>1</sub>
	CH <sub>5</sub> <sup>+</sup> + C <sub>2</sub> H <sub>2</sub> → C <sub>2</sub> H <sub>3</sub> <sup>+</sup> + CH <sub>4</sub>	1.5 × 10 <sup>-9</sup>	11	k <sub>6</sub>
C <sub>2</sub> H <sub>5</sub> <sup>+</sup>	C <sub>2</sub> H <sub>5</sub> <sup>+</sup> + e <sup>-</sup> → products	6.0 × 10 <sup>-7</sup>	31	$\alpha$ <sub>2</sub>
	C <sub>2</sub> H <sub>5</sub> <sup>+</sup> + HCN → HCNH <sup>+</sup> + C <sub>2</sub> H <sub>4</sub>	2.7 × 10 <sup>-9</sup>	30	k <sub>9</sub>
	C <sub>2</sub> H <sub>5</sub> <sup>+</sup> + C <sub>2</sub> H <sub>4</sub> → C <sub>3</sub> H <sub>5</sub> <sup>+</sup> + CH <sub>4</sub>	3.6 × 10 <sup>-10</sup>	20	k <sub>10</sub>
c-C <sub>3</sub> H <sub>3</sub> <sup>+</sup>	c-C <sub>3</sub> H <sub>3</sub> <sup>+</sup> + e <sup>-</sup> → products	3.3 × 10 <sup>-7</sup>	100	$\alpha$ <sub>4</sub>
l-C <sub>3</sub> H <sub>3</sub> <sup>+</sup>	l-C <sub>3</sub> H <sub>3</sub> <sup>+</sup> + C <sub>2</sub> H <sub>4</sub> → C <sub>5</sub> H <sub>5</sub> <sup>+</sup> + H <sub>2</sub>	5.5 × 10 <sup>-10</sup>	44	k <sub>13</sub>
	l-C <sub>3</sub> H <sub>3</sub> <sup>+</sup> + C <sub>2</sub> H <sub>4</sub> → C <sub>5</sub> H <sub>7</sub> <sup>+</sup> + h $\nu$	5.5 × 10 <sup>-10</sup>	44	k <sub>14</sub>
C <sub>3</sub> H <sub>5</sub> <sup>+</sup>	C <sub>3</sub> H <sub>5</sub> <sup>+</sup> + e <sup>-</sup> → products	3.8 × 10 <sup>-7</sup>	74	$\alpha$ <sub>3</sub>
C <sub>4</sub> H <sub>3</sub> <sup>+</sup>	C <sub>4</sub> H <sub>3</sub> <sup>+</sup> + e <sup>-</sup> → products	3.4 × 10 <sup>-7</sup>	59	$\alpha$ <sub>5</sub>
	C <sub>4</sub> H <sub>3</sub> <sup>+</sup> + C <sub>2</sub> H <sub>4</sub> → C <sub>6</sub> H <sub>5</sub> <sup>+</sup> + H <sub>2</sub>	1.2 × 10 <sup>-10</sup>	24	k <sub>20</sub>
	C <sub>4</sub> H <sub>3</sub> <sup>+</sup> + C <sub>2</sub> H <sub>2</sub> → C <sub>6</sub> H <sub>5</sub> <sup>+</sup> + h $\nu$	2.2 × 10 <sup>-10</sup>	12	k <sub>21</sub>
C <sub>5</sub> H <sub>5</sub> <sup>+</sup>	C <sub>5</sub> H <sub>5</sub> <sup>+</sup> + e <sup>-</sup> → products	3.8 × 10 <sup>-7</sup>	87	$\alpha$ <sub>6</sub>
C <sub>6</sub> H <sub>3</sub> <sup>+</sup>	C <sub>6</sub> H <sub>3</sub> <sup>+</sup> + e <sup>-</sup> → products	3.8 × 10 <sup>-7</sup>	88	$\alpha$ <sub>7</sub>
	C <sub>6</sub> H <sub>3</sub> <sup>+</sup> + C <sub>2</sub> H <sub>2</sub> → C <sub>8</sub> H <sub>5</sub> <sup>+</sup> + h $\nu$	2.3 × 10 <sup>-10</sup>	12	k <sub>26</sub>
C <sub>6</sub> H <sub>7</sub> <sup>+</sup>	C <sub>6</sub> H <sub>7</sub> <sup>+</sup> + e <sup>-</sup> → products	7.7 × 10 <sup>-7</sup>	100	$\alpha$ <sub>8</sub>
C <sub>7</sub> H <sub>5</sub> <sup>+</sup>	C <sub>7</sub> H <sub>5</sub> <sup>+</sup> + e <sup>-</sup> → products	3.8 × 10 <sup>-7</sup>	98	$\alpha$ <sub>9</sub>
C <sub>7</sub> H <sub>9</sub> <sup>+</sup>	C <sub>7</sub> H <sub>9</sub> <sup>+</sup> + e <sup>-</sup> → products	3.8 × 10 <sup>-7</sup>	100	$\alpha$ <sub>10</sub>
C <sub>8</sub> H <sub>3</sub> <sup>+</sup>	C <sub>8</sub> H <sub>3</sub> <sup>+</sup> + e <sup>-</sup> → products	3.8 × 10 <sup>-7</sup>	100	$\alpha$ <sub>11</sub>
NH <sub>4</sub> <sup>+</sup>	NH <sub>4</sub> <sup>+</sup> + e <sup>-</sup> → products	8.0 × 10 <sup>-7</sup>	100	$\alpha$ <sub>12</sub>
HCNH <sup>+</sup>	HCNH <sup>+</sup> + e <sup>-</sup> → products	1.6 × 10 <sup>-7</sup>	35	$\alpha$ <sub>13</sub>
	HCNH <sup>+</sup> + HC <sub>3</sub> N → HC <sub>3</sub> NH <sup>+</sup> + HCN	3.4 × 10 <sup>-9</sup>	34	k <sub>45</sub>
	HCNH <sup>+</sup> + C <sub>2</sub> H <sub>3</sub> CN → C <sub>2</sub> H <sub>3</sub> CNH <sup>+</sup> + HCN	4.5 × 10 <sup>-9</sup>	11	k <sub>46</sub>
CH <sub>2</sub> NH <sub>2</sub> <sup>+</sup>	CH <sub>2</sub> NH <sub>2</sub> <sup>+</sup> + e <sup>-</sup> → products	3.8 × 10 <sup>-7</sup>	100	$\alpha$ <sub>14</sub>
CH <sub>3</sub> CNH <sup>+</sup>	CH <sub>3</sub> CNH <sup>+</sup> + e <sup>-</sup> → products	1.8 × 10 <sup>-7</sup>	100	$\alpha$ <sub>15</sub>
HC <sub>3</sub> NH <sup>+</sup>	HC <sub>3</sub> NH <sup>+</sup> + e <sup>-</sup> → products	9.0 × 10 <sup>-7</sup>	96	$\alpha$ <sub>16</sub>
C <sub>2</sub> H <sub>3</sub> CNH <sup>+</sup>	C <sub>2</sub> H <sub>3</sub> CNH <sup>+</sup> + e <sup>-</sup> → products	3.8 × 10 <sup>-7</sup>	97	$\alpha$ <sub>17</sub>
C <sub>2</sub> H <sub>5</sub> CNH <sup>+</sup>	C <sub>2</sub> H <sub>5</sub> CNH <sup>+</sup> + e <sup>-</sup> → products	2.6 × 10 <sup>-7</sup>	100	$\alpha$ <sub>18</sub>
C <sub>4</sub> H <sub>3</sub> NH <sup>+</sup>	C <sub>4</sub> H <sub>3</sub> NH <sup>+</sup> + e <sup>-</sup> → products	3.8 × 10 <sup>-7</sup>	100	$\alpha$ <sub>19</sub>
C <sub>4</sub> H <sub>5</sub> NH <sup>+</sup>	C <sub>4</sub> H <sub>5</sub> NH <sup>+</sup> + e <sup>-</sup> → products	3.8 × 10 <sup>-7</sup>	100	$\alpha$ <sub>20</sub>
C <sub>x</sub> H <sub>y</sub> NH <sup>+</sup>	C <sub>x</sub> H <sub>y</sub> NH <sup>+</sup> + e <sup>-</sup> → products	3.8 × 10 <sup>-7</sup>	~100	$\alpha$ <sub>21</sub>
CH <sub>3</sub> NH <sub>3</sub> <sup>+</sup>	CH <sub>3</sub> NH <sub>3</sub> <sup>+</sup> + e <sup>-</sup> → products	3.8 × 10 <sup>-7</sup>	100	$\alpha$ <sub>22</sub>
N <sub>2</sub> H <sub>5</sub> <sup>+</sup>	N <sub>2</sub> H <sub>5</sub> <sup>+</sup> + e <sup>-</sup> → products	3.8 × 10 <sup>-7</sup>	100	$\alpha$ <sub>23</sub>
H <sub>3</sub> O <sup>+</sup>	H <sub>3</sub> O <sup>+</sup> + e <sup>-</sup> → products	2.8 × 10 <sup>-7</sup>	46	$\alpha$ <sub>24</sub>
	H <sub>3</sub> O <sup>+</sup> + HCN → HCNH <sup>+</sup> + H <sub>2</sub> O	3.8 × 10 <sup>-9</sup>	42	k <sub>74</sub>
CH <sub>3</sub> OH <sub>2</sub> <sup>+</sup>	CH <sub>3</sub> OH <sub>2</sub> <sup>+</sup> + e <sup>-</sup> → products	5.0 × 10 <sup>-7</sup>	100	$\alpha$ <sub>25</sub>
CH <sub>3</sub> CHOH <sup>+</sup>	CH <sub>3</sub> CHOH <sup>+</sup> + e <sup>-</sup> → products	3.8 × 10 <sup>-7</sup>	100	$\alpha$ <sub>26</sub>

If considering the available literature only, the major reaction producing CH<sub>2</sub>NH<sub>2</sub><sup>+</sup> in our model (60 cm<sup>-3</sup> in the observed spectrum at  $m/z = 30$ ) is reaction of CH<sub>3</sub><sup>+</sup> with NH<sub>3</sub> (k<sub>47</sub>). However, the calculated density is about 2 orders of magnitude too low. We have a good measurement of CH<sub>3</sub><sup>+</sup> from the spectrum and we know the NH<sub>3</sub> density from  $m/z = 18$  so there are not any degrees of freedom. Some reactions involving CH<sub>3</sub>NH<sub>2</sub> could produce CH<sub>2</sub>NH<sub>2</sub><sup>+</sup> if CH<sub>3</sub>NH<sub>2</sub> were present in appreciable amount (k<sub>48</sub>, k<sub>49</sub>). However, there is no detectable signal

at  $m/z = 32$ , indicating that the CH<sub>3</sub>NH<sub>3</sub><sup>+</sup> and CH<sub>3</sub>NH<sub>2</sub> densities are low. We retrieve an upper limit for the mole fraction of CH<sub>3</sub>NH<sub>2</sub> of 10<sup>-8</sup> (see Section 3.3). This density is far too small for reactions k<sub>48</sub> and k<sub>49</sub> to produce a significant amount of CH<sub>2</sub>NH<sub>2</sub><sup>+</sup>. It follows that proton transfer from protonated neutrals with lower PA than CH<sub>2</sub>NH is the major production of CH<sub>2</sub>NH<sub>2</sub><sup>+</sup> (k<sub>50</sub>, k<sub>51</sub>). We assume the main loss to be electron dissociative recombination ( $\alpha$ <sub>14</sub>) and we retrieve a mole fraction for CH<sub>2</sub>NH of 1 × 10<sup>-5</sup>.

Proton attachment to  $\text{CH}_3\text{CN}$ ,  $\text{HC}_3\text{N}$  and  $\text{C}_2\text{H}_3\text{CN}$  accounts for more than 80% of the production of  $\text{CH}_3\text{CNH}^+$  at  $m/z = 42$  ( $k_{52}$ ,  $k_{53}$ ),  $\text{HC}_3\text{NH}^+$  at  $m/z = 52$  ( $k_{54}$ ,  $k_{55}$ ), and  $\text{C}_2\text{H}_3\text{CNH}^+$  at  $m/z = 54$  ( $k_{56}$ ,  $k_{57}$ ). Experimental data are available for most of the reactions and there is little doubt about these processes. Because of the high density of these three ions in the observed spectrum ( $>50 \text{ cm}^{-3}$ ), it is difficult to imagine missing condensation or radiative association reactions that would be efficient enough to produce them. Note that  $\text{HC}_3\text{NH}^+$  had been predicted to be produced at a high rate via proton exchange reactions (Keller et al., 1998). All three species are almost exclusively lost through electron dissociative recombination ( $\alpha_{15}$ – $\alpha_{17}$ ) and we retrieve mole fractions for  $\text{CH}_3\text{CN}$ ,  $\text{HC}_3\text{N}$  and  $\text{C}_2\text{H}_3\text{CN}$  of  $3 \times 10^{-6}$ ,  $4 \times 10^{-5}$  and  $1 \times 10^{-5}$ , respectively.

The formation of  $\text{C}_2\text{H}_5\text{CNH}^+$  at  $m/z = 56$  is not as clear-cut. The main production reaction available in the literature for  $\text{C}_2\text{H}_5\text{CNH}^+$  ( $k_{58}$ ) is  $\sim 400$  times too slow. Some missing condensation reactions of hydrocarbon ions with HCN or  $\text{CH}_3\text{CN}$  producing  $\text{C}_2\text{H}_5\text{CNH}^+$  can be conceived but in the absence of data, we consider that the most likely process to produce  $\text{C}_2\text{H}_5\text{CNH}^+$  is proton attachment to  $\text{C}_2\text{H}_5\text{CN}$  ( $k_{59}$ ,  $k_{60}$ ).  $\text{C}_2\text{H}_5\text{CNH}^+$  is exclusively lost through electron dissociative recombination ( $\alpha_{18}$ ) and we retrieve a mole fraction for  $\text{C}_2\text{H}_5\text{CN}$  of  $5 \times 10^{-7}$ .

Few reactions in the database can form  $\text{C}_4\text{H}_3\text{NH}^+$  at  $m/z = 66$ . The only one that could potentially produce a large amount of this ion is the radiative association  $k_{61}$ . However, this reaction was studied in a SIFT apparatus at  $\sim 0.5$  Torr, a pressure at which the adduct is collisionally stabilized (McEwan et al., 1994). On Titan, only bimolecular radiative stabilization occurs and since this process is less efficient than collisional stabilization, the above rate constant can be considered as an upper limit. Another point regarding this reaction is that it involves the propargyl ion  $\text{l-C}_3\text{H}_3^+$ . As mentioned previously, we find a lower limit for the ratio of  $\text{l-C}_3\text{H}_3^+/\text{c-C}_3\text{H}_3^+$  of 20%. We estimate that the reaction contributes to  $\sim 20\%$  of the total density at  $m/z = 66$ , though the uncertainty in both the rate constant and the  $\text{l-C}_3\text{H}_3^+$  mole fraction must be kept in mind. Even if the mole fraction of  $\text{l-C}_3\text{H}_3^+$  is slightly higher, it does not seem that this reaction is able to account for the density at  $m/z = 66$  ( $30 \text{ cm}^{-3}$ ). Missing condensation reactions involving ions and neutrals abundant enough to reproduce the observed density do not seem to be producing this ion. As a result, it seems likely that proton transfer to  $\text{C}_4\text{H}_3\text{N}$  is the major production mechanism for  $\text{C}_4\text{H}_3\text{NH}^+$  ( $k_{62}$ ,  $k_{63}$ ). We assume  $\text{C}_4\text{H}_3\text{NH}^+$  to be exclusively lost through electron dissociative recombination ( $\alpha_{19}$ ) and we retrieve a mole fraction for  $\text{C}_4\text{H}_3\text{N}$  of  $4 \times 10^{-6}$ .

The only N-containing ion mostly formed in the model by condensation or associative reactions is  $\text{C}_4\text{H}_5\text{NH}^+$  at  $m/z = 68$  ( $k_{64}$ ). It follows that proton transfer reactions from protonated neutrals with low PA to  $\text{C}_4\text{H}_5\text{N}$  have to be negligible for the model not to overestimate the observed density at  $m/z = 68$  ( $3 \text{ cm}^{-3}$ ). We assume that  $\text{C}_4\text{H}_5\text{NH}^+$  is lost via electron dissociative recombination ( $\alpha_{20}$ ) and retrieve an upper limit of  $3 \times 10^{-7}$  for the mole fraction of  $\text{C}_4\text{H}_5\text{N}$ . Note

that this ion was predicted at a high density as well by Keller et al. (1998) but was being formed by reaction  $k_{65}$ . However, the rate constant used in the Keller et al. (1998) model is an upper limit and the actual value is probably lower. Production of  $\text{C}_4\text{H}_5\text{NH}^+$  from this reaction is not required for our model to fit  $m/z = 68$ , indicating that the rate constant must be less than  $2.0 \times 10^{-11} \text{ cm}^3 \text{ s}^{-1}$ . Another possibility is that we are missing some important loss reactions for this ion in the model.

Data on reactions generating  $\text{HC}_5\text{NH}^+$ ,  $\text{C}_5\text{H}_5\text{NH}^+$ ,  $\text{C}_6\text{H}_3\text{NH}^+$  and  $\text{C}_6\text{H}_7\text{NH}^+$  at  $m/z = 76$ , 80, 90 and 94, respectively, are very scarce. The few reactions available can only produce a few percent of the observed density at best. Many condensation reactions involving heavy hydrocarbon ions and N-bearing neutrals can possibly form these ions. However, in the absence of measurements, it appears reasonable to assume that the most efficient mechanism producing these ions is proton exchange reactions. Many isomers exist for these molecules but all present a high PA, suggesting that proton attachment is a fast process. We generalize their production channel as reactions  $k_{66}$  and  $k_{67}$  and assume their loss to occur exclusively through electron dissociative recombination ( $\alpha_{21}$ ). We retrieve mole fractions for  $\text{HC}_5\text{N}$ ,  $\text{C}_5\text{H}_5\text{N}$ ,  $\text{C}_6\text{H}_3\text{N}$  and  $\text{C}_6\text{H}_7\text{N}$  of  $1 \times 10^{-6}$ ,  $4 \times 10^{-7}$ ,  $3 \times 10^{-7}$  and  $1 \times 10^{-7}$ , respectively.

### 3.3. Non-detected species

Methylamine ( $\text{CH}_3\text{NH}_2$ ) and hydrazine ( $\text{N}_2\text{H}_4$ ) are predicted as minor species in Titan's upper atmosphere (Wilson and Atreya, 2004). Both have a high PA (Table 1) and are expected to undergo proton transfer with protonated neutrals with lower PA to create  $\text{CH}_3\text{NH}_3^+$  at  $m/z = 32$  and  $\text{N}_2\text{H}_5^+$  at  $m/z = 33$ , respectively. Since we do not detect any measurable signal at these mass-to-charge ratios, we can retrieve an upper limit for the mole fraction of these species, by using reactions  $k_{68}$  plus  $k_{69}$ , and  $k_{70}$  plus  $k_{71}$ , respectively and estimated electron recombination reactions  $\alpha_{22}$  and  $\alpha_{23}$ . For an ion density of  $0.1 \text{ cm}^{-3}$ , we retrieve an upper limit for the mole fraction of both species of  $3 \times 10^{-9}$  and  $10^{-8}$ . This is consistent with the values of  $10^{-9}$  and  $10^{-13}$  computed by Wilson and Atreya (2004) at 1100 km.

By considering a water input flux from micrometeorites, pre-Cassini models predicted the formation of  $\text{H}_3\text{O}^+$  from proton exchange reactions of  $\text{CH}_5^+$  and  $\text{C}_2\text{H}_5^+$  with  $\text{H}_2\text{O}$  (Banaszkiewicz et al., 2000; Keller et al., 1998). The ion at  $m/z = 19$  is below detection limit in the measured spectra ( $<0.2 \text{ cm}^{-3}$ ) suggesting that the mole fraction of  $\text{H}_2\text{O}$  is low. With the major production reactions  $k_{72}$  plus  $k_{73}$  and electron recombination ( $\alpha_{24}$ ) as well as reaction  $k_{74}$  as the major loss reactions, we retrieve an upper limit of  $3 \times 10^{-7}$  for  $\text{H}_2\text{O}$ .

Four other oxygen-bearing species are predicted by photochemical models as minor species in Titan's upper atmosphere (Toublanc et al., 1995; Wilson and Atreya, 2004): formaldehyde ( $\text{H}_2\text{CO}$ ), methanol ( $\text{CH}_3\text{OH}$ ), ketene ( $\text{CH}_2\text{CO}$ ) and acetaldehyde ( $\text{CH}_3\text{CHO}$ ). All these species have a high PA (Table 1) and are expected to undergo proton transfer with protonated neutrals with lower PA to create their associated ions at  $m/z = 31$ , 33, 43 and 45, respectively. The presence of  $\text{C}_2\text{H}_7^+$  and  $\text{C}_3\text{H}_7^+$

at  $m/z = 31$  and  $43$  prevents us from retrieving any information on the presence of  $\text{H}_2\text{CO}$  or  $\text{CH}_2\text{CO}$  in Titan's upper atmosphere. We do not detect any measurable signal at  $m/z = 33$  and  $45$ , indicating that the abundance of  $\text{CH}_3\text{OH}$  and  $\text{CH}_3\text{CHO}$  is low. Note that as mentioned above,  $\text{N}_2\text{H}_5^+$  would appear at  $m/z = 33$  as well. As a consequence, the sum of  $\text{CH}_3\text{OH}_2^+$  and  $\text{N}_2\text{H}_5^+$  densities is less than  $0.1 \text{ cm}^{-3}$  (Fig. 2).

We retrieve an upper limit for the mole fraction of these species, by using reactions  $k_{74}$  plus  $k_{75}$ , and  $k_{76}$  plus  $k_{77}$ , respectively and electron recombination reactions  $\alpha_{25}$  and  $\alpha_{26}$ . We find an upper limit for the mole fraction of  $\text{CH}_3\text{OH}$  and  $\text{CH}_3\text{CHO}$  of  $3 \times 10^{-8}$  and  $10^{-8}$ , respectively. This is consistent with the values of  $10^{-10}$  computed by Wilson and Atreya (2004) at 1100 km. Note that ethylene oxide (*c*- $\text{C}_2\text{H}_4\text{O}$ ), an isomer of acetaldehyde, was reported by Bernard et al. (2003) in simulation experiments. Very little is known about ion–neutral chemistry of this species. Based on acetaldehyde's and ethylene oxide's similar proton affinities (768.5 and 774.2 kJ/mol, respectively), we estimate an upper limit for ethylene oxide close to  $10^{-8}$ .

Another family of species expected in Titan's atmosphere is dicyanopolyynes of general formula  $\text{C}_n\text{N}_2$ , where  $n$  is an even integer (Lara et al., 1996; Toubanc et al., 1995; Wilson and Atreya, 2004). The low PA of the dicyanopolyynes combined with the presence of  $\text{C}_4\text{H}_5^+$  and  $\text{C}_6\text{H}_5^+$  at  $m/z = 53$  and  $77$  prevents us from retrieving any evidence of the presence of  $\text{C}_2\text{N}_2$  or  $\text{C}_4\text{N}_2$  in Titan's upper atmosphere. For the same reason, we could not identify in the spectrum any ion containing two nitrogen atoms.

### 3.4. Error analysis

Major sources of uncertainties for the neutral mole fractions arise from: (i) uncertainties in the measured ion densities, (ii) uncertainties in the ionization rate, (iii) uncertainties in the reaction list. Electron temperature and  $\text{CH}_4$  plus other hydrocarbon mixing ratios are well constrained by RPWS and INMS respectively and represent only minor sources of uncertainties.

Uncertainties in the observed ion densities are due to counting statistics and calibration. Error bars reflecting the uncertainty due to counting statistics are included in Fig. 2. They become relatively larger for low density ions but are always smaller than the systematic  $\sim 20\%$  uncertainty due to calibration. Uncertainties due to the description of the electron flux are difficult to quantify but the good agreement of the model with the observations for the primary ions suggests that they are small. A study on the propagation of the uncertainties on reaction rate constants and branching ratios in a Titan ion chemistry model found that densities of the heavier ions are uncertain by up to 110% (Carrasco et al., 2007).

Consequently, we consider that the mole fraction of the neutrals for which the chemistry is well known are uncertain by a factor of 2–3. These species are  $\text{C}_2\text{H}_4$ ,  $\text{C}_4\text{H}_2$ ,  $\text{NH}_3$ ,  $\text{HCN}$ ,  $\text{CH}_3\text{CN}$ ,  $\text{HC}_3\text{N}$ , and  $\text{C}_2\text{H}_3\text{CN}$ . Note that the mole fractions inferred for  $\text{C}_2\text{H}_4$ ,  $\text{C}_4\text{H}_2$  and  $\text{CH}_3\text{CN}$  are smaller than the mole fractions presented in Vuitton et al. (2006a) by factors of a few. This decrease is due to improvements in the chemical reaction

list, leading to more efficient proton transfer from these neutrals to the associated protonated ions.

For other mostly heavier species, the chemistry is extremely uncertain and we assumed that some ions are mainly produced via proton attachment to the neutrals and lost through electron recombination. This implies that condensation reactions, radiative association reactions or fragmentation of ions with  $m/z > 100$  are minor processes. Measurement of the rate constants and products of the N-bearing closed-shell ions mentioned in this paper with hydrocarbons is desperately needed. In the absence of evidence for such processes to occur, we believe that our approach is reasonable and do not consider it a major source of uncertainty. However, since we had to estimate the rate constants for most of these reactions, we consider that this increases the total uncertainty by an additional factor of 2. Mole fractions are then probably determined within a factor of 5.

The model cannot reproduce the observed density of a few ions. For example, the observed density at  $m/z = 50$  is underestimated by a factor of 20 by the model. This mass can be attributed to  $\text{C}_3\text{N}^+$  and  $\text{C}_4\text{H}_2^+$ , but none of these species is an abundant product of the ion–neutral chemistry. Carrasco et al. (2007) and Keller et al. (1998) predict a substantial density at  $m/z = 50$  (Figs. 1 and 9 in Carrasco et al., 2007). The large amount of  $\text{C}_2\text{H}_2$  used in these models (mole fraction of  $2\text{--}8 \times 10^{-3}$ ) is responsible for an important formation of  $\text{C}_4\text{H}_2^+$  from reaction of  $\text{C}_2\text{H}_2^+$  with  $\text{C}_2\text{H}_2$ . However, the  $\text{C}_2\text{H}_2$  density is now well constrained by the INMS observations in the neutral model (Table 1) and this reaction cannot produce enough  $\text{C}_4\text{H}_2^+$  to explain the high density at  $m/z = 50$ . Note that the density at  $m/z = 64$  is underestimated as well by the model (factor of 50). This corresponds to the addition of a  $-\text{CH}_2$  unit on the ion at  $m/z = 50$  and it can be expected that analogous pathways will produce both ions at  $m/z = 50$  and  $64$ .

The observed density at  $m/z = 63$  ( $\text{C}_5\text{H}_3^+$ ) is underestimated by one order of magnitude while the observed density at  $m/z = 57$  ( $\text{C}_4\text{H}_9^+$ ) is overestimated by one order of magnitude. As mentioned previously, the chemistry becomes very uncertain for these higher  $m/z$  and missing reactions can probably account for these discrepancies. Heavier neutrals not included in the model, such as  $\text{C}_4\text{H}_6$  and  $\text{C}_4\text{H}_{10}$  could also significantly contribute to the production/destruction of these ions.

## 4. Discussion

We have inferred the mole fraction in Titan's upper atmosphere of 7 hydrocarbons and 12 N-bearing species. In the following, we will compare our results to (i) previous observations at all levels of the atmosphere, (ii) laboratory simulations of Titan's chemistry, (iii) photochemical models of neutral chemistry and (iv) interstellar medium. This helps in identifying the structure of the molecules (isomers) and in constraining production pathways, photolysis rates and chemical reactivity.

Previous observations provide constraints on the abundance of several of the molecules identified here. The mole fractions of  $\text{C}_2\text{H}_4$ ,  $\text{HCN}$ , and  $\text{HC}_3\text{N}$  in the upper atmosphere have been inferred from the Voyager 1 solar occultation experiment (Vervack et al., 2004). The Composite InfraRed Spectrome-

Table 5  
Production yields of selected compounds detected during laboratory experiments simulating Titan's atmospheric chemistry. The production yields are relative to C<sub>2</sub>H<sub>2</sub> for hydrocarbons and relative to HCN for N-bearing species

		Thompson et al. (1991)	Coll et al. (1999)	Fujii and Arai (1999)	This work
Initial gas mixture		10% CH <sub>4</sub> , 90% N <sub>2</sub>	2% CH <sub>4</sub> , 98% N <sub>2</sub>	10% CH <sub>4</sub> , 90% N <sub>2</sub>	2% CH <sub>4</sub> , 98% N <sub>2</sub>
Pressure (mbar)		17	2	26	4 × 10 <sup>-8</sup>
Temperature (K)		300	100–150	300	150
Analytical technique		Indirect GC–MS	Indirect GC–MS	Direct Li <sup>+</sup> -MS	MS-modeling
C <sub>2</sub> H <sub>2</sub>	Acetylene	1 × 10 <sup>0</sup>	1 × 10 <sup>0</sup>	1 × 10 <sup>0</sup>	1 × 10 <sup>0</sup>
C <sub>4</sub> H <sub>2</sub>	1,3-Butadiyne	3 × 10 <sup>-3</sup>	7 × 10 <sup>-4</sup>	2 × 10 <sup>0</sup>	4 × 10 <sup>-2</sup>
C <sub>6</sub> H <sub>2</sub>	1,3,5-Hexatriyne	–	6 × 10 <sup>-6</sup>	–	3 × 10 <sup>-3</sup>
C <sub>6</sub> H <sub>6</sub>	Benzene	–	7 × 10 <sup>-4</sup>	Trace	1 × 10 <sup>-2</sup>
C <sub>7</sub> H <sub>8</sub>	Toluene	–	3 × 10 <sup>-4</sup>	–	7 × 10 <sup>-4</sup>
NH <sub>3</sub>	Ammonia	–	<sup>a</sup>	5 × 10 <sup>-1</sup>	3 × 10 <sup>-2</sup>
HCN	Hydrogen cyanide	1 × 10 <sup>0</sup>	1 × 10 <sup>0</sup>	1 × 10 <sup>0</sup>	1 × 10 <sup>0</sup>
CH <sub>2</sub> NH	Methanimine	–	–	7 × 10 <sup>-1</sup>	5 × 10 <sup>-2</sup>
CH <sub>3</sub> CN	Acetonitrile	3 × 10 <sup>-2</sup>	2 × 10 <sup>-3</sup>	3 × 10 <sup>0</sup>	2 × 10 <sup>-2</sup>
HC <sub>3</sub> N	Propiolonitrile	5 × 10 <sup>-2</sup>	5 × 10 <sup>-3</sup>	4 × 10 <sup>-1</sup>	2 × 10 <sup>-1</sup>
C <sub>2</sub> H <sub>3</sub> CN	2-Propenenitrile	8 × 10 <sup>-3</sup>	1 × 10 <sup>-3</sup>	1 × 10 <sup>0</sup>	5 × 10 <sup>-2</sup>
C <sub>2</sub> H <sub>5</sub> CN	Propanenitrile	2 × 10 <sup>-2</sup>	3 × 10 <sup>-3</sup>	2 × 10 <sup>0</sup>	3 × 10 <sup>-3</sup>
C <sub>3</sub> H <sub>3</sub> CN	2-Butynenitrile	5 × 10 <sup>-4</sup>	9 × 10 <sup>-5</sup>	5 × 10 <sup>-1</sup>	2 × 10 <sup>-2</sup>
HC <sub>5</sub> N	Pentadiynenitrile	–	4 × 10 <sup>-6</sup>	–	5 × 10 <sup>-3</sup>
C <sub>4</sub> H <sub>5</sub> CN	2,4-Pentadienenitrile	5 × 10 <sup>-5</sup>	7 × 10 <sup>-6</sup>	–	2 × 10 <sup>-3</sup>
	2-Methylene-3-butenenitrile	3 × 10 <sup>-5</sup>	–	–	2 × 10 <sup>-3</sup>
C <sub>5</sub> H <sub>7</sub> CN	2,4-Hexadienenitrile?	6 × 10 <sup>-5</sup>	2 × 10 <sup>-5</sup>	–	5 × 10 <sup>-4</sup>

<sup>a</sup> NH<sub>3</sub> was identified later on by Bernard et al. (2003) with the same experimental conditions.

ter (CIRS) on Cassini retrieves stratospheric abundance vertical profiles of C<sub>2</sub>H<sub>4</sub>, C<sub>4</sub>H<sub>2</sub>, C<sub>6</sub>H<sub>6</sub>, HCN and HC<sub>3</sub>N (Teanby et al., 2006; Vinatier et al., 2007). Ground-based microwave spectroscopy provides constraints on the upper stratospheric abundance of HCN, CH<sub>3</sub>CN, HC<sub>3</sub>N, C<sub>2</sub>H<sub>3</sub>CN, C<sub>2</sub>H<sub>5</sub>CN and HC<sub>5</sub>N (Marten et al., 2002). Neutral mole fractions at 300 km are listed in Table 1. Comparison of our results to these datasets provides density vertical profiles of the species that help constrain their altitude of formation.

Laboratory experiments relevant to the atmospheric chemistry induced in Titan's atmosphere by saturnian magnetospheric electrons have been performed. Typically, a mixture of a few mbar of CH<sub>4</sub> in N<sub>2</sub> is flowing in a cold plasma discharge. The products are subsequently analyzed by an analytical procedure generally based on mass spectrometry and the production yield of each species is determined. In order to compare this value with the INMS results, we scale the production yields to C<sub>2</sub>H<sub>2</sub> for the hydrocarbons and to HCN for the N-bearing species. Results and experimental conditions for a subset of the laboratory simulation experiments are presented in Table 5.

Coll et al. (1999) use the most representative gas mixture and temperature. Because of experimental limitations, the pressure in all three experiments is orders of magnitude higher than in Titan's upper atmosphere. In Coll et al. (1999) and Thompson et al. (1991) experiments, the products are collected in a cold trap and subsequently transferred to the analytical system while Fujii and Arai (1999) analyze the products in real time. Note the systematic higher yield of N-bearing species relative to HCN observed by Fujii and Arai (1999). The reason is that their technique of Li<sup>+</sup> ion association depends markedly on the number of atoms in the neutral molecule. The rate of attachment of Li<sup>+</sup>

to HCN is very much slower than to the larger nitriles hence the ratios measured always favor the larger molecules (Edwards et al., 2006). Laboratory simulations results are further compared with our results on Titan's atmosphere below.

Photochemical models of Titan's neutral chemistry extending from the surface to the upper atmosphere have been developed (Lara et al., 1996; Toublanc et al., 1995; Yung et al., 1984). Recent models also include a subset of ion–molecule chemistry in the upper atmosphere (Banaszkiewicz et al., 2000; Wilson and Atreya, 2004). The models describe the chemical and physical processes taking place in the atmosphere, and compute the vertical profiles of the chemical compounds. Neutral mole fractions obtained at 1100 km are listed in Table 6. Comparison of our results to these predictions provides a test for the reaction set used in the models and helps constrain the production and loss pathways for the chemical species.

It is interesting to note that most of the species identified in this work have already been observed in the interstellar (ISM) and circumstellar medium. The ISM is a very complex environment, with wide differences in densities, gas composition, temperature and energy sources. It is not our goal here to perform a thorough review of the abundance of molecules in the different parts of the ISM. Even for a single source, observations are scattered and it is often difficult to reconcile line of sight abundances obtained by different teams, with different telescopes, different data reduction techniques, etc. Instead, we focused on two objects known as good organic chemistry factories for which consistent sets of data were acquired: the Taurus Molecular Cloud (TMC-1) and the proto-planetary nebula CRL 618. TMC-1 is a prototypical dark cloud with a kinetic temperature of 10 K that contains a number of differ-

Table 6  
Neutral mole fractions of selected compounds at 1100 km computed by photochemical models

	Yung et al. (1984)	Toublanc et al. (1995)	Banaszkiewicz et al. (2000)	Wilson and Atreya (2004) <sup>a</sup>	This work
C <sub>2</sub> H <sub>4</sub>	6 × 10 <sup>-3</sup>	3 × 10 <sup>-3</sup>	2 × 10 <sup>-3</sup>	1 × 10 <sup>-3</sup>	1 × 10 <sup>-3</sup>
C <sub>4</sub> H <sub>2</sub>	8 × 10 <sup>-5</sup>	6 × 10 <sup>-6</sup>	2 × 10 <sup>-5</sup>	2 × 10 <sup>-6</sup>	1 × 10 <sup>-5</sup>
C <sub>6</sub> H <sub>2</sub>	4 × 10 <sup>-6</sup>	2 × 10 <sup>-8</sup>	–	1 × 10 <sup>-8</sup>	8 × 10 <sup>-7</sup>
C <sub>6</sub> H <sub>6</sub>	–	–	–	1 × 10 <sup>-10</sup>	3 × 10 <sup>-6</sup>
C <sub>8</sub> H <sub>2</sub>	2 × 10 <sup>-7</sup>	1 × 10 <sup>-9</sup>	–	5 × 10 <sup>-11</sup>	2 × 10 <sup>-7</sup>
HCN	2 × 10 <sup>-3</sup>	5 × 10 <sup>-4</sup>	3 × 10 <sup>-3</sup>	9 × 10 <sup>-4</sup>	2 × 10 <sup>-4</sup>
CH <sub>3</sub> CN	–	4 × 10 <sup>-9</sup>	7 × 10 <sup>-6</sup>	1 × 10 <sup>-5</sup>	3 × 10 <sup>-6</sup>
C <sub>2</sub> H <sub>3</sub> CN	–	–	–	1 × 10 <sup>-6</sup>	1 × 10 <sup>-5</sup>
HC <sub>3</sub> N	1 × 10 <sup>-4</sup>	5 × 10 <sup>-6</sup>	7 × 10 <sup>-6</sup>	2 × 10 <sup>-6</sup>	4 × 10 <sup>-5</sup>
NH <sub>3</sub>	–	–	–	4 × 10 <sup>-8</sup>	7 × 10 <sup>-6</sup>

<sup>a</sup> Values for solar minimum conditions.

ent carbon-chain sequences, including the cyanopolynes, the methylcyanopolynes and the methylpolynes. CRL 618 is a carbon-rich proto-planetary nebula (C/O > 1), with kinetic temperatures between 200 and 250 K in the region where the molecules are observed.

#### 4.1. Unsaturated N-bearing species

We inferred the presence of NH<sub>3</sub> in Titan's upper atmosphere, with a mole fraction of 7 × 10<sup>-6</sup> (Table 1). Although not previously detected on Titan (upper limit of 6.3 × 10<sup>-9</sup> in the stratosphere), NH<sub>3</sub> has been produced in laboratory experiments simulating Titan's conditions (Bernard et al., 2003; Fujii and Arai, 1999), and a photochemical model predicts its presence in the upper atmosphere (Wilson and Atreya, 2004), although at a low density (mole fraction of 4 × 10<sup>-8</sup>).

In the Wilson and Atreya (2004) model, production of NH<sub>3</sub> in the ionosphere occurs via initial formation of NH<sub>4</sub><sup>+</sup> and its subsequent electron recombination to NH<sub>3</sub>. The mechanism, first proposed in Atreya (1986), consists of an initial reaction of N<sup>+</sup> with H<sub>2</sub> giving NH<sup>+</sup>, followed by successive reactions of NH<sub>n</sub><sup>+</sup> (n = 1, 2, 3) with H<sub>2</sub> and CH<sub>4</sub>. However, because of the low density of H<sub>2</sub> in Titan's atmosphere, the initial reaction produces only a small concentration of NH<sup>+</sup> (7.0 × 10<sup>-3</sup> cm<sup>-3</sup>) in our model and this pathway is only responsible for 1% of our NH<sub>4</sub><sup>+</sup> production. This is consistent with Wilson and Atreya (2004) underestimating by 2 orders of magnitude, the NH<sub>3</sub> abundance. Another pathway suggested by these authors involves the recombination of H atoms and NH<sub>2</sub> radicals. However, this process requires a collision with a third body and is not efficient at the low pressure of the upper atmosphere (10<sup>-7</sup> mbar).

NH<sub>3</sub> is ubiquitous in the ISM where it is formed on grain surfaces by consecutive addition of H atoms onto NH (Lequeux, 2005). NH radicals are readily available only in the upper atmosphere on Titan. Data from the UltraViolet Spectrometer (UVIS) onboard Cassini seems to show some evidence for the presence of haze up to 750 km and maybe higher (Liang et al., 2007). If this is confirmed, heterogeneous chemistry taking place at the surface of the aerosols might be the key to the formation of NH<sub>3</sub> on Titan.

We inferred the presence of CH<sub>2</sub>NH in Titan's upper atmosphere, with a mole fraction of 1 × 10<sup>-5</sup> (Table 1). Although not previously detected on Titan, CH<sub>2</sub>NH has been produced in a laboratory experiment simulating Titan's conditions (Fujii and Arai, 1999). CH<sub>2</sub>NH is observed in the ISM, where it is formed by gas-phase chemistry as well as on grain surfaces (Dickens et al., 1997).

A single photochemical model considers CH<sub>2</sub>NH as a product of Titan's atmospheric chemistry (Lara et al., 1996). A CH<sub>2</sub>NH production only ~6 times lower than the HCN production is calculated. Unfortunately, its fate after production is not followed and its abundance cannot be retrieved. In this model, it is assumed that CH<sub>2</sub>NH is formed in the reaction between NH and CH<sub>3</sub>. It was recently confirmed that CH<sub>2</sub>NH is indeed the major product in this reaction (Redondo et al., 2006). The reaction between N(<sup>2</sup>D) and CH<sub>4</sub> could also contribute to the formation of CH<sub>2</sub>NH (Herron, 1999) since both species are abundant in Titan's upper atmosphere. As a consequence, CH<sub>2</sub>NH should be a significant product of the neutral chemistry. Heterogeneous chemistry could also contribute to the formation of CH<sub>2</sub>NH if aerosols are present in the upper atmosphere. It may be presumed that CH<sub>2</sub>NH is lost by photolysis and/or condensation.

NH<sub>3</sub> and CH<sub>2</sub>NH are the first two N-containing species detected on Titan for which the N atom is not sequestered in a –C≡N group. This is particularly interesting since the N atom is available to further react and produce more complex species. For example, polymerization of CH<sub>2</sub>NH at low temperature to produce a cyclic trimer (hexahydro-1,3,5-triazine) has been suggested in model interstellar icy grain mantles (Bernstein et al., 1995).

#### 4.2. Saturated nitriles

We inferred the presence in the upper atmosphere of three saturated nitriles, HCN, CH<sub>3</sub>CN, and C<sub>2</sub>H<sub>5</sub>CN. The mole fraction of HCN determined in our analysis (2 × 10<sup>-4</sup>) is in good agreement with the value inferred from the Voyager 1 solar occultation experiment, although obtained at 100 km lower altitude (Verhock et al., 2004). CIRS measurements at 80° N show a steady decrease in HCN mole fraction from 10<sup>-5</sup> to 10<sup>-6</sup> between 500 and 300 km (Vinatier et al., 2007). Ground-based mi-

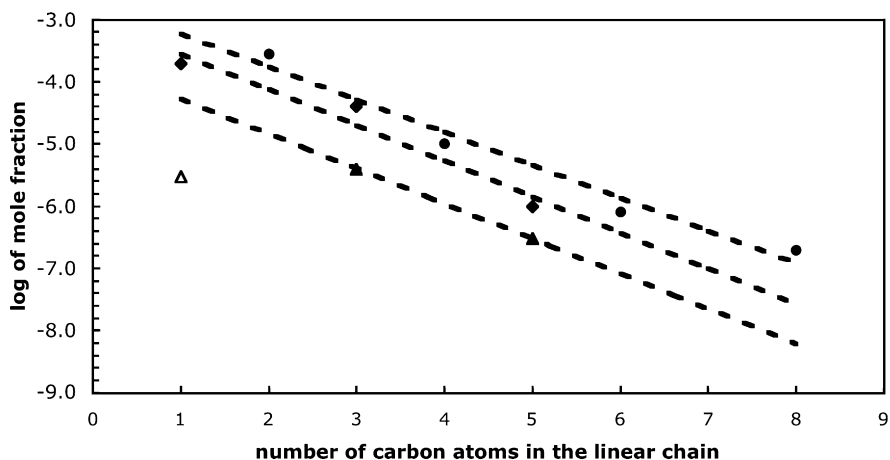


Fig. 4. Plot of the logarithm (base 10) of the mole fractions of polyynes ( $C_nH_2$ , circles), cyanopolyynes ( $HC_mN$ , diamonds) and methylcyanopolyynes ( $CH_3C_nN$ , triangles) versus the number of carbon atoms in the linear chain ( $n, m$ ) as retrieved using our ion chemistry model. The dashed lines result from a fit to the data and their slopes are presented in Table 5. The mole fraction of  $CH_3CN$  is not included in the fit and is represented by an open triangle.

crowave spectroscopy provides a disk average mole fraction at 450 km of  $8 \times 10^{-7}$  and  $4 \times 10^{-8}$  for HCN and  $CH_3CN$  respectively and an upper limit of  $2 \times 10^{-9}$  for  $C_2H_5CN$  (Marten et al., 2002). These values are a factor of  $\sim 200$  smaller than those derived in the upper atmosphere. The fact that all 3 species present about the same gradient from upper to lower atmosphere indicates that their evolution is closely related. This is fully consistent with production in the upper atmosphere and diffusion to lower altitudes, where loss occurs through chemistry and condensation.

The three nitriles are ubiquitous in laboratory experiments as shown in Table 5 (Coll et al., 1999; Fujii and Arai, 1999; Thompson et al., 1991). As mentioned earlier, the higher yields of  $CH_3CN$  and  $C_2H_5CN$  found by Fujii and Arai (1999) are attributed to the  $Li^+$  attachment technique. All three species are observed in various sources in the ISM (Lequeux, 2005). Photochemical models (Banaszkiewicz et al., 2000; Toubanc et al., 1995; Wilson and Atreya, 2004; Yung et al., 1984) tend to overestimate the HCN mole fraction by a factor of a few. Banaszkiewicz et al. (2000) and Toubanc et al. (1995) predict a  $CH_3CN$  mole fraction that is 3 orders of magnitude too small. Wilson and Atreya (2004) calculate a  $CH_3CN$  mole fraction in agreement with our value, with insertion of  $N(^2D)$  into  $C_2H_4$  being the major production reaction. None of the photochemical models consider  $C_2H_5CN$ . In the ISM, the reaction of protonated ethanol with HCN followed by electron recombination is thought to be the main  $C_2H_5CN$  source (Charnley, 1997). On Titan, ethyl cation transfer to HCN is probably not important since species having a PA higher than HCN have a low density. Formation pathways similar to those forming  $CH_3CN$  such as insertion of  $N(^2D)$  into  $C_3H_6$  can be expected. This reaction will have to be included in future models.

#### 4.3. Polyne families

Polyynes are species with general formula  $C_nH_2$  ( $n$  is an even integer) that are separated by 24 amu. We inferred the presence in Titan's upper atmosphere of the 4 first members of this family, with mole fractions presented in Table 1.

$C_4H_2$  is ubiquitous in laboratory experiments simulating Titan's conditions and is produced at a yield relative to  $C_2H_2$  of about  $10^{-3}$  as showed in Table 5 (Coll et al., 1999; Thompson et al., 1991). The high  $C_4H_2/C_2H_2$  ratio obtained by Fujii and Arai (1999) probably reflects the slow attachment of  $Li^+$  to  $C_2H_2$  compared to the larger molecule  $C_4H_2$ .  $C_6H_2$  has been observed in experiments performed at low temperature (100–150 K) (Coll et al., 1999). Photochemical models predict the formation of polyne chains through neutral chemistry pathways, with a maximum production around 800 km (Toubanc et al., 1995; Wilson and Atreya, 2004; Yung et al., 1984). Formation in the thermosphere is consistent with the observed 3 orders of magnitude decrease in  $C_4H_2$  mole fraction from 1100 to 300 km (Coustenis et al., 1989; Vinatier et al., 2007).  $C_2H_2$ ,  $C_4H_2$  and  $C_6H_2$  have been detected in the direction of the protoplanetary nebula CRL 618 (Cernicharo et al., 2001).

The logarithm of the mole fractions of  $C_nH_2$  as retrieved using our ion chemistry model is plotted as circles in Fig. 4. The slope of the line that results from a fit to the data is presented in Table 7. The same slope as computed from the yields in laboratory experiments, from the predictions of photochemical models at 1100 km and from the observations in CRL 618 are presented in Table 7 as well. We find that the mole fraction of the polyynes inferred from the INMS data decreases with increasing number of carbon atoms at a rate 2 to 4 times slower than predicted by photochemical models (Toubanc et al., 1995; Wilson and Atreya, 2004; Yung et al., 1984) and about 6 times slower than produced in laboratory simulations (Coll et al., 1999).  $C_6H_2$  and to a lesser extent  $C_4H_2$  tend to polymerize rapidly at room temperature and might be lost during transfer to the analytical device. On the contrary, they decrease at a rate 2.5 faster than in CRL 618. In photochemical models dedicated to Titan, polyne growth is initiated with their photodissociation followed by insertion of the radical formed:

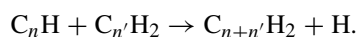
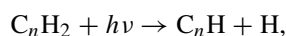


Table 7

The slope of the logarithm (base 10) of the mole fractions of polyynes ( $C_nH_2$ ), cyanopolyynes ( $HC_mN$ ), methylpolyynes ( $CH_3C_nH$ ) and methylcyanopolyynes ( $CH_3C_mN$ ) versus the number of carbon atoms in the linear chain ( $n, m$ ), as computed in photochemical models, as measured in laboratory experiments, as observed in CRL 618 and TMC-1 and as retrieved using our ion chemistry model. The range of the number of carbon atoms used to perform the fit is showed in parenthesis

Species	Photochemical models			Laboratory experiments	ISM		This work
	Yung et al. (1984)	Toublanc et al. (1995)	Wilson and Atreya (2004)		TMC-1	CRL 618	
$C_nH_2$	-0.76 (2–8)	-1.07 (2–8)	-1.18 (2–8)	-1.30 (2–6)	–	-0.13 (2–6)	-0.53 (2–8)
$HC_mN$	–	–	–	-1.34 (1–5)	-0.27 (3–9)	-0.18 (1–7)	-0.58 (1–5)
$CH_3C_nH$	–	–	–	–	-0.36 (2–6)	–	–
$CH_3C_mN$	–	–	–	–	-0.23 (1–5)	–	-0.56 (3, 5)

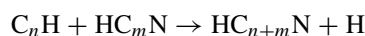
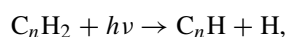
Similar processes are used to explain the presence of polyynes in the ISM.

Earlier Titan models relied mostly on data obtained in pyrolysis conditions that were extrapolated to Titan's conditions (Toublanc et al., 1995; Yung et al., 1984). Recent experiments performed at low temperature show that  $C_2H$  actually reacts about 4 times faster than assumed in these models (Chastaing et al., 1998; Lee et al., 2000; Vakhtin et al., 2001). Other recent data include low temperature measurements of the absorption cross sections of  $C_2H_2$ ,  $C_4H_2$  and  $C_6H_2$  and photolysis quantum yields of  $C_2H_2$  (Bénilan et al., 1995, 2000; Läuter et al., 2002; Smith et al., 1998). These studies indicate an increased production rate of  $C_2H$  from  $C_2H_2$  photolysis and updated models should lead to a more efficient formation of the higher polyynes than is currently computed, in agreement with our results (Table 7). Other laboratory measurements required to improve photochemical models include rate constants for  $C_4H$  (and heavier) radicals as well as photolysis branching ratios for  $C_4H_2$  and heavier polyynes (Vuitton et al., 2006b).

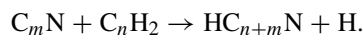
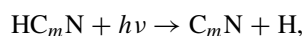
We define cyanopolyynes as species with general formula  $HC_mN$ , where  $m$  is an odd integer. We inferred the presence in the upper atmosphere of the first 3 members of this family, HCN,  $HC_3N$  and  $HC_5N$ .  $HC_3N$  is ubiquitous in laboratory experiments but its yield relative to HCN varies by 2 orders of magnitude as showed in Table 5 (Coll et al., 1999; Fujii and Arai, 1999; Thompson et al., 1991).  $HC_5N$  is not stable at 300 K but has been observed in low temperature (100–150 K) experiments (Coll et al., 1999). Cyanopolyne chains containing up to 7 and 11 carbon atoms have been observed in CRL 618 and TMC-1, respectively (Cernicharo et al., 2001; Remijan et al., 2006).

The logarithm of the mole fractions of  $HC_mN$  as retrieved using our ion chemistry model is plotted as diamonds in Fig. 4. The slope of the line that results from a fit to the data is presented in Table 7. The same slope, as computed from the yields in laboratory experiments and from the observations in CRL 618 and TMC-1 are presented in Table 7 as well. Whatever this slope is, it is striking to see that the mole fraction of polyynes and cyanopolyynes decreases with increasing number of carbon at an almost identical rate in laboratory experiments, Titan's atmosphere and the proto-planetary nebula. This is consistent with the fact that they are structurally similar (an H atom is

replaced by a CN group) and are formed through similar pathways:



and/or



In Titan photochemical models, the production peak arises around 800 km, consistent with an observed 3 orders of magnitude higher mole fraction at 1100 km than at 300 km (Coustenis et al., 1989; Teanby et al., 2006). However, photochemical models systematically underestimate our inferred  $HC_3N$  density at 1100 km by a factor of a few (Banaszkiewicz et al., 2000; Toublanc et al., 1995; Wilson and Atreya, 2004), probably because of the lack of data on the photodissociation and kinetics of the species involved. Formation of cyanopolyynes other than  $HC_3N$  has not been quantified so far, but these species have been considered in polymer-producing schemes (Lebonnois et al., 2002; Wilson and Atreya, 2003).

We inferred the presence of  $C_7H_4$  from the observation of  $C_7H_5^+$  at  $m/z = 89$ .  $C_5H_5^+$  at  $m/z = 65$  is efficiently formed through condensation reactions and we could only retrieve an upper limit for the mole fraction of  $C_5H_4$ . None of these species have been observed in laboratory simulations or included in photochemical models. However both methyl diacetylene ( $CH_3C_4H$ ) and methyl triacetylene ( $CH_3C_6H$ ) have been observed in TMC-1 (Remijan et al., 2006; Walmsley et al., 1984). The mole fraction of methylpolyynes decreases with increasing number of carbon at a rate similar within experimental uncertainties to the rate of polyynes and cyanopolyynes (Table 7), suggesting that the mechanism of forming the three carbon-chain sequences are highly correlated. With two data points only and the large uncertainty in the mole fraction of  $C_7H_4$ , it was not possible to constrain a trend in the growth process of methylpolyynes on Titan. However, the data do not disagree with the slope observed for polyynes and cyanopolyynes.

It has been shown that the reaction between the ethynyl radical,  $C_2H$ , and methylacetylene, yields two  $C_5H_4$  isomers, methyl diacetylene ( $CH_3C_4H$ ) and to a minor amount ethynylallene ( $H_2C_3H(C_2H)$ ) (Stahl et al., 2002). The reaction is fast

(Hoobler and Leone, 1999),  $C_2H$  and  $CH_3C_2H$  are present in Titan's upper atmosphere, and these species should be a significant product of the neutral chemistry. Similarly,  $C_4H$  could react with  $CH_3C_2H$  and/or  $C_2H$  with  $CH_3C_4H$  to produce the  $C_7H_4$  isomers.

We inferred the presence of  $C_4H_3N$  and  $C_6H_3N$  from the observation of  $C_4H_3NH^+$  and  $C_6H_3NH^+$  at  $m/z = 66$  and  $90$ . Methylcyanoacetylene,  $CH_3C_3N$ , is ubiquitous in laboratory experiments (Coll et al., 1999; Fujii and Arai, 1999; Thompson et al., 1991). Its high yield in the Fujii and Arai (1999) experiment is again a bias introduced by the  $Li^+$  attachment technique (Table 5).  $C_6H_3N$  has never been observed in such experiments. Neither  $C_4H_3N$  nor  $C_6H_3N$  has been included in photochemical models. Both  $C_4H_3N$  and  $C_6H_3N$  have been observed in TMC-1 (Brotten et al., 1984; Lovas et al., 2006; Snyder et al., 2006). It is interesting to note that two isomers of  $C_4H_3N$  were identified and that cyanoallene ( $CH_2CCHCN$ ) was found to be  $\sim 4.5$  times more abundant than the more stable form, methylcyanoacetylene ( $CH_3C_3N$ ). When it comes to  $C_6H_3N$ , only methylcyanodiacetylene ( $CH_3C_5N$ ) has been detected so far.

The reaction between  $CN + CH_3C_2H$  is fast (Carty et al., 2001) and produces in collisionless conditions both  $C_4H_3N$  isomers, methylcyanoacetylene and cyanoallene (Balucani et al., 2000). The detection of both isomers in TMC-1 and the observation that the mole fraction of  $C_4H_3N$  and  $C_6H_3N$  decreases with increasing numbers of carbon at a rate almost identical as the rate inferred for cyanopolynes (Table 7) strongly suggests that this reaction is responsible for the formation of  $C_4H_3N$  in TMC-1. The same trend is seen in Titan's atmosphere as well (Fig. 4, Table 7).  $CN$  and  $CH_3C_2H$  are present in Titan's upper atmosphere and as a consequence  $CH_3C_3N$  and  $H_2C_3(CN)H$  should be a significant product of the neutral chemistry. Similar reactions involving heavier hydrocarbons or  $C_3N$  radicals could produce  $C_6H_3N$ .

#### 4.4. Other N-bearing species

We inferred the presence of  $C_2H_3CN$  in Titan's upper atmosphere, with a mole fraction of  $1 \times 10^{-5}$  (Table 1). Although not previously detected on Titan,  $C_2H_3CN$  is produced in laboratory experiments simulating Titan's conditions (Coll et al., 1999; Fujii and Arai, 1999; Thompson et al., 1991), and is predicted by neutral chemistry models (Lebonnois et al., 2002; Wilson and Atreya, 2004). In the Wilson and Atreya (2004) model, production of  $C_2H_3CN$  occurs mainly in the upper atmosphere ( $\sim 1000$  km) via the reaction between  $CN$  and  $C_2H_4$ . This high altitude production is in agreement with the sharp decrease in  $C_2H_3CN$  density from the upper to the lower atmosphere, where an upper limit of  $2.0 \times 10^{-9}$  has been retrieved (Marten et al., 2002). However, the Wilson and Atreya (2004) prediction for  $C_2H_3CN$  at 1100 km is too low by a factor of  $\sim 10$ .  $C_2H_3CN$  has been detected in various sources outside the Solar System (Lequeux, 2005).

The total rate constant of the reaction between  $CN$  and  $C_2H_4$  is well established, even at low temperature (Herbert et al., 1992; Sims et al., 1993). However, branching fractions for the

2 possible channels ( $C_2H_3CN + H$  and  $C_2H_3 + HCN$ ) are not. Wilson and Atreya (2004) assume from Monks et al. (1993) a branching fraction of 0.2 for the channel forming  $C_2H_3CN$ . However, more recent experiments suggested that the branching fraction to  $C_2H_3CN$  is close to 1 (Balucani et al., 2000; Choi et al., 2004). This is an interesting possibility since it would increase the formation of  $C_2H_3CN$  at the expense of  $HCN$ , which is slightly overestimated by Wilson and Atreya (2004). This hypothesis will have to be tested in future models.

From the ion densities at  $m/z = 80$  and  $94$ , we infer the presence of a few tenths of a ppm of  $C_5H_5N$  and  $C_6H_7N$  in Titan's upper atmosphere. In their laboratory simulation, Thompson et al. (1991) observe the formation of 2 isomers of  $C_5H_5N$ , penta-2,4-dienitrile and 2-methylene-3-butenitrile, the former being observed by Coll et al. (1999) as well. Both groups detect a  $C_6H_7N$  species, that Thompson et al. (1991) tentatively attribute to 2,4-hexadienenitrile. However, many other isomers are possible, including cycles such as pyridine ( $C_5H_5N$ ) and aniline ( $C_6H_5NH_2$ ). Neither species has been detected in any extraterrestrial object. Clearly, new processes are required to explain their presence in Titan's upper atmosphere.

#### 4.5. Aromatic hydrocarbons

We infer the presence in the upper atmosphere of a few ppm of  $C_6H_6$ . This is in good agreement with the detection of  $C_6H_6$  obtained by INMS in the neutral mode for low-altitude flybys (Vuitton et al., 2007). Benzene has been observed in various laboratory experiments (Coll et al., 1999; Fujii and Arai, 1999). Wilson et al. (2003) and Wilson and Atreya (2004) find that the primary mechanism responsible for the benzene formation is the recombination of propargyl ( $C_3H_3$ ) radicals, with ion chemistry being the principal source of benzene molecules in the upper atmosphere. However, these processes only lead to a benzene mole fraction of  $10^{-8}$  at the production peak (750 km) and  $10^{-10}$  at 1100 km, 3 orders of magnitude lower than observed by INMS. Lebonnois (2005), in a sensitivity study of benzene production in Titan's atmosphere, obtains a mole fraction of benzene up to  $10^{-5}$  at the production peak, decreasing to a few  $10^{-7}$  at 1100 km. However, this result is obtained with a propargyl self-reaction rate of  $1.2 \times 10^{-10} \text{ cm}^3 \text{ s}^{-1}$  (Mortier et al., 1994). Three very recent studies at 295 K report a three times lower rate coefficient that supersedes the former value (Atkinson and Hudgens, 1999; De Sain and Taatjes, 2003; Fahr and Nayak, 2000). Using this lower rate leads only to a 20–50 percent decrease of benzene according to Lebonnois (2005).

Benzene production pathways are generally based on studies dedicated to combustion conditions that are poorly relevant to Titan. For example, the recombination rate for propargyl radicals has never been measured below room temperature or in its low-pressure range. The low-pressure rate constant is then generally assumed to be equal to 10 times the recombination rate of methyl ( $CH_3$ ) radicals because of the higher number of channels available to redistribute the excess energy. A faster rate could significantly enhance the benzene mole fraction in the upper atmosphere. However, the large abundance in the ther-

mosphere implies that  $C_6H_6$  is created in the upper atmosphere. This strongly suggests that  $C_6H_6$  is most likely created by a 2-body process. For example, the reaction between  $C_2H$  and butadiene (1,3- $C_4H_6$ ) is fast ( $k = 3 \times 10^{-10} \text{ cm}^3 \text{ s}^{-1}$ ) and butadiene is efficiently produced in the recombination of  $C_2H_3$  radicals (Fahr et al., 1991; Nizamov and Leone, 2004). The products have not been determined but it is usually believed that the reaction of  $C_2H$  with unsaturated molecules proceeds via attack of a  $\pi$ -orbital followed by rapid loss of an H atom by the energized complex initially formed, to form a  $C_6H_6$  molecule in this case.

Large polycyclic aromatic hydrocarbons (PAHs) have been proposed as the carriers of the unidentified interstellar bands (UIBs), but identification of specific PAH molecules outside the Solar System has been elusive. Only recently has benzene been detected in the direction of the proto-planetary nebula CRL 618. Polymerization of acetylene induced by the UV photons coming from the hot central star or by the shocks associated with its high-velocity winds may be prominently involved in the formation of benzene (Cernicharo et al., 2001). The  $C_2H_2/C_6H_6$  ratio observed in CRL 618 and in Titan's upper atmosphere is of the same order of magnitude ( $\sim 40$  and  $\sim 90$ , respectively) and it is possible similar production pathways induced by UV photons occur in both environments. Note that shocks do not occur on Titan.

We infer the presence of a few tenths of a ppm of  $C_7H_8$  in Titan's upper atmosphere. Toluene is an aromatic ring with a methyl group. This species is produced in laboratory experiments simulating Titan's conditions (Coll et al., 1999) but has not been included in photochemical models. It has not been observed in any extraterrestrial object to date. No gas phase reactions that could explain the presence of toluene in Titan's atmosphere have been proposed so far. Its production from the addition of  $CH_3$  and  $C_6H_5$  radicals has been shown to be quite efficient ( $k = 2 \times 10^{-11} \text{ cm}^3 \text{ s}^{-1}$ ) at room temperature and a few Torr pressure (Tokmakov et al., 1999). Another reaction possibly forming toluene is the addition of  $C_3H_3$  and  $C_4H_5$  radicals. Studies at low temperature and pressure are required in order to evaluate the efficiency of these processes in Titan's upper atmosphere.

#### 4.6. Oxygen-bearing species

Three oxygen-bearing species have been detected in Titan's lower stratosphere, namely  $CO$ ,  $CO_2$  and  $H_2O$ , with mole fractions of  $\sim 5 \times 10^{-5}$  (Flasar et al., 2005; Gurwell and Muhleman, 1995),  $\sim 2 \times 10^{-8}$  (Coustenis et al., 1989; Flasar et al., 2005) and  $\sim 8 \times 10^{-9}$  (Coustenis et al., 1998), respectively. While the origin of  $CO$  is not clear, it is believed that  $H_2O$  is injected into Titan's upper atmosphere by the ablation of micrometeorites.  $OH$  radicals subsequently produced by the photolysis of  $H_2O$  react with  $CO$  to form  $CO_2$ . Photochemical models require a downward flux of about  $3 \times 10^6 \text{ cm}^2 \text{ s}^{-1}$   $H_2O$  molecules (referred to the surface) in order to reproduce the observed  $CO_2$  and  $H_2O$  mixing ratios (Coustenis et al., 1998; Lara et al., 1996). This value is consistent with ablation models that compute  $H_2O$  deposition rates in the Saturn system

(English et al., 1996; Feuchtgruber et al., 1997). However, with such a rate, photochemical models predict a  $H_2O$  mole fraction of a few  $10^{-5}$  at 1100 km. The upper limit retrieved here from the INMS ion spectrum for  $H_2O$  is 2 orders of magnitude lower. This implies that the  $H_2O$  deposition rate inferred by Lara et al. (1996) has to be revised. New photochemical models with updated transport and oxygen chemistry are required to settle this issue.

## 5. Conclusion

We developed an ion-chemistry model in order to analyze INMS ion spectra obtained during the T5 flyby of Titan by the Cassini spacecraft. We identified the major ions present in Titan's upper atmosphere and we showed that their density directly depends on the composition of the neutral atmosphere. It follows that coupling measurement of the ion densities to our chemical model allows us to infer the mole fraction of 19 neutrals in Titan's upper atmosphere with mole fractions ranging from  $10^{-7}$  to  $10^{-3}$ . They represent far more complex molecules than previously thought.

We detect polyynes ( $C_4H_2$ ,  $C_6H_2$ ,  $C_8H_2$ ) and cyanopolyynes ( $HC_3N$ ,  $HC_5N$ ) with densities orders of magnitude higher than predicted by photochemical models (Toublanc et al., 1995; Wilson and Atreya, 2004; Yung et al., 1984). Our results also indicate the probable presence of methylcyanopolyynes ( $CH_3C_3N$ ,  $CH_3C_5N$ ) and maybe methylpolyynes ( $CH_3C_4H$ ,  $CH_3C_6H$ ), species that are observed in the interstellar medium (Brotten et al., 1984; MacLeod et al., 1984; Remijan et al., 2006; Snyder et al., 2006; Walmsley et al., 1984) but that had never really been considered for Titan. The data also suggests the presence of ammonia ( $NH_3$ ), methanimine ( $CH_2NH$ ), other nitriles ( $C_2H_3CN$ ,  $C_2H_5CN$ ) and two unidentified N-containing species ( $C_5H_5N$ ,  $C_6H_7N$ ). Finally, we confirm the detection by INMS in the neutral mode of benzene ( $C_6H_6$ ) (Vuitton et al., 2007). Photochemical models do not reproduce the observed abundance or do not even predict the presence of these molecules in Titan's atmosphere (Lara et al., 1996;oublanc et al., 1995; Wilson and Atreya, 2004; Yung et al., 1984). Note that all these species are highly unsaturated, consistent with the 12 amu periodicity observed in the ion spectrum.

Comparison of our results in the upper atmosphere with available observations in the stratosphere (Marten et al., 2002; Teanby et al., 2006; Vinatier et al., 2007) show a strong density gradient from 300 to 1100 km for all the species. This confirms the prediction of photochemical models that unsaturated hydrocarbons and N-containing species are mainly formed in the upper atmosphere. However, the current incapacity of photochemical models to better match the observations reflects a dramatic lack of kinetic data in the low temperature and pressure conditions of Titan's upper atmosphere.

Only exothermic reactions can take place in Titan's cold environment and above 800 km, the chemistry is mostly driven by highly energetic radicals such  $CH$ ,  $C_2H$ ,  $N(^2D)$  or  $CN$ . Radical recombination reactions are very exothermic but they require collisions with a third body to transfer the excess energy. The

pressure dependence of this process is not well constrained for most reactions, especially at low temperature. Photochemical models generally use values extrapolated from the low-pressure rate constant for methyl–methyl recombination. However, this rate is itself uncertain by up to 2 orders of magnitude at 150 K (Moses et al., 2000). It follows that it is extremely difficult to establish the altitude dependence of 3-body reaction rates in Titan's atmosphere. If these reactions are still efficient at lower pressure than is currently assumed, the production rate of complex species through 3-body reactions could be significantly enhanced and shifted to higher altitudes.

Banaszkiewicz et al. (2000) find that when ion chemistry is included in their model, the density of  $C_2H_2$ ,  $C_4H_2$  and HCN increases by a factor of about 3 and that the density of  $C_3H_4$  increases by about one order of magnitude. This suggests that ion–molecule chemistry can significantly contribute to the formation of neutrals in the upper atmosphere. This process probably occurs through electron recombination reactions. More experimental data on electron recombination rates for a wide range of electron temperature and on reaction products, especially for heavier hydrocarbon ions and N-containing ions are crucial for the understanding of Titan's ionospheric chemistry.

The species discussed here include the most complex molecules identified so far on Titan. This confirms the long-thought idea that a very rich chemistry is actually taken place in this atmosphere. These molecules are possibly the first intermediates in the formation of even larger molecules. Consequently, Titan provides us with a unique opportunity to understand how large organic molecules are formed. Polynes, cyanopolynes, acrylonitrile and benzene have been suggested as precursors in the formation of Titan's aerosols (Lebonnois et al., 2002; Wilson and Atreya, 2003). Aerosols influence all levels of the atmosphere through radiative transfer as well as the surface appearance and composition. Note that the region of maximum aerosol production obtained by photochemical models is lower than required by microphysical models (150–200 km versus 200–400 km). It is doubtful that dynamical effects could explain this discrepancy alone. Considering the higher density of aerosol precursors in the upper atmosphere would certainly help solving this problem. Further studies constraining the rate and altitude of production of the species inferred here is then of primary importance.

The measurements presented here are a snapshot of Titan's upper atmosphere at a particular altitude, latitude and local time. We analyzed the T5 INMS ion spectra obtained at closest approach (1027–1200 km) but measurements were obtained with a good signal to noise ratio up to 1600 km (Cravens et al., 2006). Above 1200 km, diffusion cannot be neglected and developing a one-dimensional photochemical model is required in order to retrieve altitude profiles for the neutral species presented here. Such profiles should shed some light on the altitude of formation of the species and consequently on their formation processes. Finally, analysis of more recent flybys obtained at a different latitude and/or solar zenith angle will provide some information on the dynamics and energy deposition processes in Titan's upper atmosphere.

## Acknowledgments

We thank T. Cravens, R. Thissen, O. Dutuit, A. Somogyi, H. Imanaka and M. Smith for useful discussion of Titan chemistry. This work has been supported by the NASA Grant NAG5-12699 to the University of Arizona and by the Cassini–Huygens project.

## Supplementary material

The online version of this article contains additional supplementary material.

Please visit DOI: [10.1016/j.icarus.2007.06.023](https://doi.org/10.1016/j.icarus.2007.06.023).

## References

- Anicich, V.G., McEwan, M.J., 1997. Ion–molecule chemistry in Titan's ionosphere. *Planet. Space Sci.* 45, 897–921.
- Anicich, V.G., Wilson, P.F., McEwan, M.J., 2006. An ICR study of ion–molecule reactions in Titan's atmosphere: An investigation of binary hydrocarbon mixtures up to 1 micron. *J. Am. Soc. Mass Spectrom.* 17, 544–561.
- Atkinson, D.B., Hudgens, J.W., 1999. Rate coefficients for the propargyl radical self-reaction and oxygen addition reaction measured using ultraviolet cavity ring-down spectroscopy. *J. Phys. Chem. A* 103, 4242–4252.
- Atreya, S.K., 1986. *Atmospheres and Ionospheres of the Outer Planets and Their Satellites*. Springer-Verlag, New York.
- Balucani, N., Asvany, O., Osamura, Y., Huang, L.C.L., Lee, Y.T., Kaiser, R.I., 2000. Laboratory investigation on the formation of unsaturated nitriles in Titan's atmosphere. *Planet. Space Sci.* 48, 447–462.
- Banaszkiewicz, M., Lara, L.M., Rodrigo, R., Lopez-Moreno, J.J., Molina-Cuberos, G.J., 2000. A coupled model of Titan's atmosphere and ionosphere. *Icarus* 147, 386–404.
- Bénilan, Y., Bruston, P., Raulin, F., Courtin, R., Guillemin, J.C., 1995. Absolute absorption coefficient of  $C_6H_2$  in the mid-UV range at low temperature: Implications for the interpretation of Titan atmospheric spectra. *Planet. Space Sci.* 43, 83–89.
- Bénilan, Y., Smith, N., Jolly, A., Raulin, F., 2000. The long wavelength range temperature variations of the mid-UV acetylene absorption coefficient. *Planet. Space Sci.* 48, 463–471.
- Bernard, J.-M., Coll, P., Coustenis, A., Raulin, F., 2003. Experimental simulation of Titan's atmosphere: Detection of ammonia and ethylene oxide. *Planet. Space Sci.* 51, 1003–1011.
- Bernstein, M.P., Sandford, S.A., Allamandola, L.J., Chang, S., Scharberg, M.A., 1995. Organic compounds produced by photolysis of realistic interstellar and cometary ice analogs containing methanol. *Astrophys. J.* 454, 327–344.
- Brotten, N.W., MacLeod, J.M., Avery, L.W., Irvine, W.M., Höglund, B., Friberg, P., Hjalmarsen, Å., 1984. The detection of interstellar methylcyanoacetylene. *Astrophys. J.* 276, L25–L29.
- Carrasco, N., Dutuit, O., Thissen, R., Banaszkiewicz, M., Pernot, P., 2007. Uncertainty analysis of bimolecular reactions in Titan ionosphere chemistry model. *Planet. Space Sci.* 55, 141–157.
- Carty, D., Le Page, V., Sims, I.R., Smith, I.W.M., 2001. Low temperature rate coefficients for the reactions of CN and  $C_2H$  radicals with allene and methyl acetylene. *Chem. Phys. Lett.* 344, 310–316.
- Cernicharo, J., Heras, A.M., Tielens, A.G.G.M., Pardo, J.R., Herpin, F., Guélin, M., Waters, L.B.F.M., 2001. Infrared Space Observatory's discovery of  $C_4H_2$ ,  $C_6H_2$ , and benzene in CRL 618. *Astrophys. J.* 546, L123–L126.
- Charnley, S.B., 1997. On the nature of interstellar organic chemistry. In: *Cosmochimica Acta*, Eds. C.B., Bowyer, S., Werthimer, D. (Eds.), *Astronomical and Biochemical Origins and the Search for Life in the Universe*. Editrice Compositori, Bologna, pp. 89–96.
- Chastaing, D., James, P.L., Sims, I.R., Smith, I.W.M., 1998. Neutral–neutral reactions at the temperatures of interstellar clouds. Rate coefficients for reactions of  $C_2H$  radicals with  $O_2$ ,  $C_2H_2$ ,  $C_2H_4$  and  $C_3H_6$  down to 15 K. *Faraday Discuss.* 109, 165–181.

- Choi, N., Blitz, M.A., McKee, K., Pilling, M.J., Seakins, P.W., 2004. H atom branching ratios from the reactions of CN radicals with  $C_2H_2$  and  $C_2H_4$ . *Chem. Phys. Lett.* 384, 68–72.
- Coll, P., Coscia, D., Smith, N., Gazeau, M.-C., Ramirez, S.I., Cernogora, G., Israel, G., Raulin, F., 1999. Experimental laboratory simulation of Titan's atmosphere: Aerosols and gas phase. *Planet. Space Sci.* 47, 1331–1340.
- Coustenis, A., Bézard, B., Gautier, D., 1989. Titan's atmosphere from Voyager infrared observations. I. The gas composition of Titan's equatorial region. *Icarus* 80, 54–76.
- Coustenis, A., Salama, A., Lellouch, E., Encrenaz, T., Bjoraker, G.L., Samuelson, R.E., de Graauw, T., Feuchtgruber, H., Kessler, M.F., 1998. Evidence for water vapor in Titan's atmosphere from ISO/SWS data. *Astron. Astrophys.* 336, L85–L89.
- Cravens, T.E., and 15 colleagues, 2006. Composition of Titan's ionosphere. *Geophys. Res. Lett.* 33, doi:10.1029/2005GL025575. L07105.
- De Sain, J.D., Taatjes, C.A., 2003. Infrared laser absorption measurements of the kinetics of propargyl radical self-reaction and the 193 nm photolysis of propyne. *J. Phys. Chem. A* 107, 4843–4850.
- Dickens, J.E., Irvine, W.M., De Vries, C.H., Ohishi, M., 1997. Hydrogenation of interstellar molecules: A survey for methylenimine ( $CH_2NH$ ). *Astrophys. J.* 479, 307–312.
- Edwards, S.J., Freeman, C.G., McEwan, M.J., Wilson, P.F., 2006. A selected ion flow tube investigation of the gas phase chemistry of  $Li^+$ . *Int. J. Mass Spectrom.* 255/256, 164–169.
- English, M., Lara, L.M., Lorenz, R.D., Ratcliff, P.M., Rodrigo, R., 1996. Ablation and chemistry of meteoric materials in the atmosphere of Titan. *Adv. Space Res.* 17, 157–160.
- Fahr, A., Nayak, A., 2000. Kinetics and products of propargyl ( $C_3H_3$ ) radical self-reactions and propargyl–methyl cross-combination reactions. *Int. J. Chem. Kinet.* 32, 118–124.
- Fahr, A., Laufer, A.H., Klein, R., Braun, W., 1991. Reaction rate determinations of vinyl radical reactions with vinyl, methyl, and hydrogen atoms. *J. Phys. Chem.* 95, 3218–3224.
- Feuchtgruber, H., Lellouch, E., de Graauw, T., Bézard, B., Encrenaz, T., Griffin, M., 1997. External supply of oxygen to the atmospheres of the giant planets. *Nature* 389, 159–162.
- Flasar, F.M., and 19 colleagues, 2005. Titan's atmospheric temperatures, winds, and composition. *Science* 308, 975–978.
- Fox, J.L., Yelle, R.V.P., 1997. Hydrocarbon ions in the ionosphere of Titan. *Geophys. Res. Lett.* 24, 2179–2182.
- Fujii, T., Arai, N., 1999. Analysis of N-containing hydrocarbon species produced by a  $CH_4/N_2$  microwave discharge: Simulation of Titan's atmosphere. *Astrophys. J.* 519, 858–863.
- Gurwell, M.A., Muhleman, D.O., 1995. CO on Titan: Evidence for a well-mixed vertical profile. *Icarus* 117, 375–382.
- Herbert, L., Smith, I.W.M., Spencer-Smith, R.D., 1992. Rate constants for the elementary reactions between CN radicals and  $CH_4$ ,  $C_2H_6$ ,  $C_2H_4$ ,  $C_3H_6$ , and  $C_2H_2$  in the range: 295–700 K. *Int. J. Chem. Kinet.* 24, 791–802.
- Herron, J.T.E., 1999. Evaluated chemical kinetics data for reactions of  $N(^2D)$ ,  $N(^2P)$ , and  $N_2(A^3\Sigma_u^+)$  in the gas phase. *J. Phys. Chem. Ref. Data* 28, 1453–1483.
- Hoobler, R.J., Leone, S.R., 1999. Low-temperature rate coefficients for reactions of the ethynyl radical ( $C_2H$ ) with  $C_3H_4$  isomers methylacetylene and allene. *J. Phys. Chem. A* 103, 1342–1346.
- Hunter, E.P., Lias, S.G., 1998. Evaluated gas phase basicities and proton affinities of molecules: An update. *J. Phys. Chem. Ref. Data* 27, 413–656.
- Ip, W.H., 1990. Titan's upper ionosphere. *Astrophys. J.* 362, 354–363.
- Keller, C.N., Cravens, T.E., Gan, L., 1992. A model of the ionosphere of Titan. *J. Geophys. Res.* 97, 12117–12135.
- Keller, C.N., Anicich, V.G., Cravens, T.E., 1998. Model of Titan's ionosphere with detailed hydrocarbon ion chemistry. *Planet. Space Sci.* 46, 1157–1174.
- Lara, L.M., Lellouch, E., Lopez-Moreno, J.J., Rodrigo, R., 1996. Vertical distribution of Titan's atmospheric neutral constituents. *J. Geophys. Res.* 101, 23261–23283.
- Läuter, A., Lee, K.S., Jung, K.H., Vatsa, R.K., Mittal, J.P., Volpp, H.-R., 2002. Absolute primary H atom quantum yield measurements in the 193.3 and 121.6 nm photodissociation of acetylene. *Chem. Phys. Lett.* 358, 314–319.
- Lebonnois, S., 2005. Benzene and aerosol production in Titan and Jupiter's atmospheres: A sensitivity study. *Planet. Space Sci.* 53, 486–497.
- Lebonnois, S., Bakes, E.L.O., McKay, C.P., 2002. Transition from gaseous compounds to aerosols in Titan's atmosphere. *Icarus* 159, 505–517.
- Lee, S., Samuels, D.A., Hoobler, R.J., Leone, S.R., 2000. Direct measurements of rate coefficients for the reaction of ethynyl radical ( $C_2H$ ) with  $C_2H_2$  at 90 and 120 K using a pulsed Laval nozzle apparatus. *J. Geophys. Res.* 105, 15085–15090.
- Lequeux, J., 2005. *The Interstellar Medium*. Springer, Berlin.
- Liang, M.-C., Yung, Y.L., Shemansky, D.E., 2007. Photolytically generated aerosols in the mesosphere and thermosphere of Titan. *Astrophys. J.* 661, L199–L202.
- Lovas, F.J., Remijan, A.J., Hollis, J.M., Jewell, P.R., Snyder, L.E., 2006. Hyperfine structure identification of interstellar cyanoallene toward TMC-1. *Astrophys. J.* 637, L37–L40.
- MacLeod, J.M., Avery, L.W., Broten, N.W., 1984. The detection of interstellar methylidyne ( $CH_3C_4H$ ). *Astrophys. J.* 282, L89–L92.
- Marten, A., Hidayat, T., Biraud, Y., Moreno, R., 2002. New millimeter heterodyne observations of Titan: Vertical distributions of nitriles HCN,  $HC_3N$ ,  $CH_3CN$ , and the isotopic ratio  $^{15}N/^{14}N$  in its atmosphere. *Icarus* 158, 532–544.
- McEwan, M.J., Anicich, V.G., 2007. Titan's ion chemistry: A laboratory perspective. *Mass Spectrom. Rev.* 26, 281–319.
- McEwan, M.J., McConnell, C.L., Freeman, C.G., Anicich, V.G., 1994. Reactions of isomeric  $C_3H_3^+$  ions: A combined low pressure-high pressure study. *J. Phys. Chem.* 98, 5068–5073.
- Monks, P.S., Romani, P.N., Nesbitt, F.L., Scanlon, M., Stief, L.J., 1993. The kinetics of the formation of nitrile compounds in the atmospheres of Titan and Neptune. *J. Geophys. Res.* 98, 17115–17122.
- Morter, C.L., Farhat, S.K., Adamson, J.D., Glass, G.P., Curl, R.F., 1994. Rate constant measurement of the recombination reaction  $C_3H_3 + C_3H_3$ . *J. Phys. Chem.* 98, 7029–7035.
- Moses, J.I., Bézard, B., Lellouch, E., Gladstone, G.R., Feuchtgruber, H., Allen, M., 2000. Photochemistry of Saturn's atmosphere. I. Hydrocarbon chemistry and comparisons with ISO observations. *Icarus* 143, 244–298.
- Niemann, H.B., and 17 colleagues, 2005. The abundances of constituents of Titan's atmosphere from the GC-MS instrument on the Huygens probe. *Nature* 438, 779–784.
- Nizamov, B., Leone, S.R., 2004. Kinetics of  $C_2H$  reactions with hydrocarbons and nitriles in the 104–296 K temperature range. *J. Phys. Chem. A* 108, 1746–1752.
- Orient, O.J., Srivastava, S.K., 1987. Electron impact ionization of  $H_2O$ ,  $CO$ ,  $CO_2$  and  $CH_4$ . *J. Phys. B At. Mol. Opt. Phys.* 20, 3923–3936.
- Rapp, D., Englander-Golden, P., 1965. Total cross sections for ionization and attachment in gases by electron impact. I. Positive ionization. *J. Chem. Phys.* 43, 1464–1479.
- Redondo, P., Pauzat, F., Ellinger, Y., 2006. Theoretical survey of the  $NH + CH_3$  potential energy surface in relation to Titan atmospheric chemistry. *Planet. Space Sci.* 54, 181–187.
- Remijan, A.J., Hollis, J.M., Snyder, L.E., Jewell, P.R., Lovas, F.J., 2006. Methyltriacetylene ( $CH_3C_6H$ ) toward TMC-1: The largest detected symmetric top. *Astrophys. J.* 643, L37–L40.
- Sims, I.R., Queffelec, J.-L., Travers, D., Rowe, B.R., Herbert, L.B., Karthaus, J., Smith, I.W.M., 1993. Rate constants for the reactions of CN with hydrocarbons at low and ultra-low temperatures. *Chem. Phys. Lett.* 211, 461–468.
- Smith, N.S., Bénilan, Y., Bruston, P., 1998. The temperature dependent absorption cross sections of  $C_4H_2$  at mid ultraviolet wavelengths. *Planet. Space Sci.* 46, 1215–1220.
- Snyder, L.E., Hollis, J.M., Jewell, P.R., Lovas, F.J., Remijan, A.J., 2006. Confirmation of interstellar methylcyanodiacetylene ( $CH_3C_5N$ ). *Astrophys. J.* 647, 412–417.
- Stahl, F., Schleyer, P.V.R., Schaefer III, H.F., Kaiser, R.I., 2002. Reactions of ethynyl radicals as a source of  $C_4 + C_5$  hydrocarbons in Titan's atmosphere. *Planet. Space Sci.* 50, 685–692.
- Szego, K., and 19 colleagues, 2005. The global plasma environment of Titan as observed by Cassini Plasma Spectrometer during the first two close encounters with Titan. *Geophys. Res. Lett.* 32, doi:10.1029/2005GL022646. L20S05.
- Teany, N.A., and 11 colleagues, 2006. Latitudinal variations of HCN,  $HC_3N$ , and  $C_2N_2$  in Titan's stratosphere derived from Cassini CIRS data. *Icarus* 181, 243–255.

- Thompson, W.R., Henry, T.J., Schwartz, J.M., Khare, B.N., Sagan, C., 1991. Plasma discharge in  $N_2 + CH_4$  at low pressures: Experimental results and applications to Titan. *Icarus* 90, 57–73.
- Tokmakov, I.V., Park, J., Gheysa, S., Lin, M.C., 1999. Experimental and theoretical studies of the reaction of the phenyl radical with methane. *J. Phys. Chem. A* 103, 3636–3645.
- Toublanc, D., Parisot, J.P., Brillet, J., Gautier, D., Raulin, F., McKay, C.P., 1995. Photochemical modeling of Titan's atmosphere. *Icarus* 113, 2–26.
- Vakhtin, A.B., Heard, D.E., Smith, I.W.M., Leone, S.R., 2001. Kinetics of reactions of  $C_2H$  radical with acetylene,  $O_2$ , methylacetylene, and allene in a pulsed Laval nozzle apparatus at  $T = 103$  K. *Chem. Phys. Lett.* 344, 317–324.
- Vervack, R.J.J., Sandel, B.R., Strobel, D.F., 2004. New perspectives on Titan's upper atmosphere from a reanalysis of the Voyager 1 UVS solar occultations. *Icarus* 170, 91–112.
- Vinatier, S., Bézard, B., Fouchet, T., Teanby, N.A., de Kok, R., Irwin, P.G.J., Conrath, B.J., Nixon, C.A., Romani, P.N., Flasar, F.M., Coustenis, A., 2007. Vertical abundance profiles of hydrocarbons in Titan's atmosphere at  $15^\circ$  S and  $80^\circ$  N retrieved from Cassini/CIRS spectra. *Icarus* 188, 120–138.
- Vuitton, V., Yelle, R.V., Anicich, V.G., 2006a. The nitrogen chemistry of Titan's upper atmosphere revealed. *Astrophys. J.* 647, L175–L178.
- Vuitton, V., Doussin, J.-F., Bénilan, Y., Raulin, F., Gazeau, M.-C., 2006b. Experimental and theoretical study of hydrocarbon photochemistry applied to Titan stratosphere. *Icarus* 185, 287–300.
- Vuitton, V., Yelle, R.V., Cui, J., 2007. Formation and distribution of benzene on Titan. *J. Geophys. Res.*, submitted for publication.
- Waite, J.H., and 21 colleagues, 2005. Ion Neutral Mass Spectrometer results from the first flyby of Titan. *Science* 308, 982–986.
- Walmsley, C.M., Jewell, P.R., Snyder, L.E., Winniewisser, G., 1984. Detection of interstellar methylidyne ( $CH_3C_4H$ ) in the dark dust cloud TMC-1. *Astron. Astrophys.* 134, L11–L14.
- Wilson, E.H., Atreya, S.K., 2003. Chemical sources of haze formation in Titan's atmosphere. *Planet. Space Sci.* 51, 1017–1033.
- Wilson, E.H., Atreya, S.K., 2004. Current state of modeling the photochemistry of Titan's mutually dependent atmosphere and ionosphere. *J. Geophys. Res.* 109, doi:10.1029/2003JE002181. E06002.
- Wilson, E.H., Atreya, S.K., Coustenis, A., 2003. Mechanisms for the formation of benzene in the atmosphere of Titan. *J. Geophys. Res.* 108, doi:10.1029/2002JE001896. 5014.
- Yelle, R.V., Borggren, N., de la Haye, V., Kasprzak, W.T., Niemann, H.B., Müller-Wodarg, I.C.F., Waite, J.H.J., 2006. The vertical structure of Titan's upper atmosphere from Cassini Ion Neutral Mass Spectrometer measurements. *Icarus* 182, 567–576.
- Yung, Y.L., 1987. An update of nitrile photochemistry on Titan. *Icarus* 72, 468–472.
- Yung, Y.L., Allen, M., Pinto, J.P., 1984. Photochemistry of the atmosphere of Titan: Comparison between model and observations. *Astrophys. J. Suppl. Ser.* 55, 465–506.